1ST INTERNATIONAL CONFERENCE ON PHONONIC CRYSTALS, METAMATERIALS & OPTOMECHANICS

Extended Abstracts

Track 1: Phononic Crystals

Phononics 2011: First International Conference on Phononic Crystals, Metamaterials and Optomechanics
Santa Fe, New Mexico, USA, May 29-June 2, 2011
PHONONICS-2011-0024

Phononic Crystals to Control the Propagation of Elastic Waves: Recent Advances

Bernard Bonello, Laurent Belliard, Juliette Pierre, Mathieu Rénier, Olga Boyko

Institut des NanoSciences de Paris (INSP) UMR CNRS 7588,
Université Pierre et Marie Curie, boîte 840
4 place Jussieu, 75252 Paris cedex 05, France
bernard.bonello@insp.jussieu.fr, laurent.belliard@upmc.fr, juliette.pierre@insp.jussieu.fr,
mathieu.renier@insp.jussieu.fr, olga.boyko@insp.jussieu.fr

Abstract: In this paper, we briefly review the recent advances made worldwide to control the propagation of elastic waves using phononic crystals (PCs). We show how new effects, including the opening of band gaps in silicon PC plates and the negative refraction of elastic waves, could be at the origin of new Micro ElectroMechanical Systems compatible with CMOS processes.

The most attractive property that can be achieved in a phononic crystal (PC) is the existence of frequency bands in which no acoustic waves are allowed to propagate. It is thus not surprising that, since more than twenty years, a great deal of work has been devoted to the computation of the band structures of a large variety of PCs, including solid/fluid and solid/solid heterostructures. The research in this field has now reached maturity and several devices based upon the intrinsic properties of PCs have been proposed already, some of which being of primary interest for communication technologies (filters, waveguides, resonators, (de)multiplexers, signal processing devices…) or more generally, for manipulating the propagation or the focusing of elastic waves (gradient index PCs, acoustical super-lenses…). This paper presents an overview of recent works on the topics. We mostly, but not exclusively, stress on recent advances made with PCs inserted within slabs or membranes which have the important advantage of confining the elastic energy in the thickness of the device, yielding therefore to low loss structures.

The first experimental demonstration[1,2] of stop bands in 2D PC goes back to the early 70's but it is only recently that PCs in silicon plates, compatible with CMOS process, have been achieved at high frequencies. For instance, a decreasing in the transmission by almost 40 dB was measured in a PC designed to stop all plate modes in the band 120-150 MHz and elaborated[3] from a silicon-on-insulator substrate. Rejection of bulk acoustic waves by 25 dB was also measured in the MHz regime with PCs made of tungsten rods embedded into a silica matrix.[4] In both cases these stop bands resulted from the Bragg reflection on the inclusions. Actually, other processes can be exploited as well to achieve a large decrease in the transmission through the heterostructure, at specific frequencies. Indeed, it has been shown[5] that a very selective filter is obtained when a resonant cavity is attached to a waveguide arranged within a 2D PC. In that case, the dip in the transmission spectrum does not result from the coherent scattering of the waves but rather from the trapping of elastic energy in the cavity. However, up to now the experimental demonstrations have been limited to structures with fluid background, not really useable for RF applications.

Almost the same idea is at work in the case of PCs made of periodic array of dots on a membrane. These structures have at least two features being of primary usefulness for MEMS devices: first, not surprisingly, they exhibit band gaps due to Bragg reflection on the dots but also, more unexpectedly, they feature flat bands at frequencies that could be well below the Bragg gap. These low frequency gaps originate from the confinement of elastic energy on the dots and are therefore very sensitive to their geometrical and physical parameters. Secondly, the elaboration of this new type of phononic plates is compatible with CMOS processes, making these heterostructures very promising in a large field of applications (sensing, wireless communication, thermal transport…) and consequently, widely investigated worldwide.[6-10]

Phononics 2011: First International Conference on Phononic Crystals, Metamaterials and Optomechanics

Santa Fe, New Mexico, USA, May 29-June 2, 2011

PHONONICS-2011-0024

With the rapid growing of information and communication technologies there is an urgent need in frequency selective devices working in the GHz range. Various micromechanical 2D resonators showing Q-factor as high as $6x10^3$ have been proposed to this end.[11] In particular, a silicon-chip-based cavity, allowing for the simultaneous confinement of mechanical and optical modes, has recently been used[12] to successfully couple 2 GHz phonons and light at telecom wavelength (1.5 μm).

The optical approach has inspired a lot of works devoted to the bending, focusing, or collimation of elastic waves at both micro- (MHz) and nano-scales (GHz). Particularly interesting is a flat gradient-index PC lens[13] that has been designed to focus bulk elastic waves at wavelengths much larger than the lattice parameter. This could be achieved by modulating either the radii or the physical nature of the cylindrical inclusions, along the direction normal to the wave vector. It has also been shown by our group that, as a consequence of the folding of some branches in the dispersion curves, both SAW[14] and Lamb waves[15] can undergo negative refraction when going across the interface between a PC and a homogeneous medium. Identical properties could be achieved with locally resonant materials[16] as well, but in this latter case, the phenomenon results from mass density and compressibility both negative rather than from dispersion. Note that most of the investigations in that field are still prospective but they could eventually lead to very interesting devices, as super-lenses, suitable to overcome the diffraction limit when focusing an ultrasonic beam.

In summary, an abundant literature covers now many aspects of PCs as a basis to micromechanical, or microelectronic devices. In this talk, we will try to identify which of them are the most promising.

References

[1] H. J. Shutherland and R. Lingle, *J. Composite Materials* **6**, 490 (1972).
[2] T. R. Trauchert and A. N. Guzetsu, *J. Appl. Mech.* **39**, 98 (1972).
[3] S. Mohammadi, A. A. Eftekhar, A. Khelif, W. D. Hunt, and A. Adibi, *Appl. Phys. Lett.* **92**, 221905 (2008).
[4] I. El-Kady, R. H. Olsson III, and J. G. Fleming, *Appl. Phys. Lett.* **92**, 233504 (2008).
[5] J. O. Vasseur, M. Beaugeois, B. Djafari-Rouhani, Y. Pennec, and P. A. Deymier, *Phys. Stat. Sol. (c)* **1**, 2720 (2004).
[6] Y. Pennec, B. Djafari-Rouhani, H. Larabi, A. Akjouj, J. N. Gillet, J. O. Vasseur, and G. Thabet, *Phys. Rev. B* **80**, 144302 (2009).
[7] A. Khelif, Y. Achaoui, S. Benchabane, and V. Laude, *Phys. Rev. B* **81**, 214303 (2010).
[8] M. Oudich, Y. Li, B. Assouar, Z. Hou, *New Journal of Physics* **12**, 083049 (2010).
[9] T.-T. Wu, Z.-G. Huang, T.-C. Tsai, and T.-C. Wu, *Appl. Phys. Lett.* **93**, 111902 (2008).
[10] J.-C. Hsu and T. T. Wu, *Appl. Phys. Lett.* **90**, 201904 (2007).
[11] S. Mohammadi, A. A. Eftekhar, W. D. Hunt, and A. Adibi, *Appl. Phys. Lett.* **94**, 051906 (2009).
[12] M. Eichenfield, J. Chan, R. M. Camacho, K. J. Vahala, and O. Painter, *Nature* **462**, 78 (2009).
[13] Sz-C. S. Lin, T. J. Huang, J.-H. Sun, and T. T. Wu, *Phys. Rev. B* **79**, 094302 (2009).
[14] B. Bonello, L. Belliard, J. Pierre, O. Boyko, B. Perrin, J. O. Vasseur, *Phys. Rev. B* **82**, 104109 (2010).
[15] J. Pierre, O. Boyko, L. Belliard, J. O. Vasseur, B. Bonello, *Appl. Phys. Lett*. **97**, 121919 (2010).
[16] Z. Liu, X. Zhang, Y. Mao, Y. Y. Zhu, Z. Yang, C. T. Chan, and P. Sheng, *Science* **289**, 1734 (2000).

Phononics 2011: First International Conference on Phononic Crystals, Metamaterials and Optomechanics
Santa Fe, New Mexico, USA, May 29-June 2, 2011
PHONONICS-2011-0040

Band Gap Calculation for 2D Solid-Fluid Phononic Crystals by the Method Based on Dirichlet-to-Neumann Map

Xiao-Zhou Zhou[1], Ni Zhen[1], Yue-Sheng Wang[1], Chuanzeng Zhang[2]

[1] *Institute of Engineering Mechanics, Beijing Jiaotong University, Beijing 100044, China*
zhouzhou_buaa@163.com
[2] *Department of Civil Engineering, University of Siegen, D-57068 Siegen, Germany*
c.zhang@uni-siegen.de

Abstract: A method based on the Dirichlet-to-Neumann map which relates the potential function to its derivatives on the boundary of the unit cell is presented for the phononic band gap calculation with solids stuffing in a fluid. The transverse mode existing in the solid stuffing is considered. The band structures along the irreducible Brillouin zone are calculated. The results show that the method can yield accurate results with fast convergence.

Since the pioneer work of Kushwaha [1], a great deal of attention has been focused on special properties of the so-called phononic crystals [1-11] which are the artificial periodic elastic materials with the structures analogy to traditional natural crystals and photonic crystals. A physical character of these materials is the existence of phononic band gaps in which the sound or elastic waves are forbidden.

To calculate the band gaps for phononic crystals, several numerical methods have been developed, such as the plane wave expansion (PWE) method [1-6], the multiple scattering theory (MST) method [7, 8], and the finite difference time domain (FDTD) method [9, 10]. Among them, the PWE method is the most popular one because of its simplicity. For the systems with solid stuffing in a fluid, PWE method has to neglect the transverse mode existing in solid stuffing and simply treat the solid as an artificial "fluid". This approximation can yield accurate results only when the solid component is so stiff that the wave propagating in the surrounding fluid can hardly be transmitted into the solid. Up to now, there are few efficient numerical methods for calculating the band structures of the mixed system with solid and fluid components [11].

In this paper, a method based on the Dirichlet-to-Neumann (DtN) map [12] which relates the potential function to its derivatives on the boundary of the unit cell is presented for the band gap calculation of the phononic crystals with solid stuffing in a fluid. The boundary conditions between the solid stuffing and the fluid host as well as the transverse mode existing in the solid stuffing are considered. This method expresses the scattered fields as the cylindrical wave expansions and imposes the Bloch condition on the boundary of the unit cell. A linear eigenvalue equation is obtained. For a given frequency, the Bloch wave vectors along the irreducible Brillouin zone are calculated. This method is applied to analyze the band gaps of two-dimensional solid-fluid phononic crystals with a square lattice. The results show that the method can yield accurate results with fast convergence for various material combinations, including the case with soft stuffing.

As an example, a square lattice of aluminium (Al) cylinders in a mercury host with filling fraction $f = 0.4$ is considered. The material properties are $\rho_1 = 2700 kg/m^3$ and $c_{L1} = 6410 m/s$ for Al, and $\rho_2 = 13600 kg/m^3$ and $c_{L2} = 1451 m/s$ for mercury. The normalized frequencies $\bar{\omega}$ are calculated by both PWE and DtN-based methods, see Fig. 1 For the PWE method the solid stuffing is considered as a fluid but with the material parameters of actual Al. In the figure, the black circular dots represent the band structures obtained from the DtN-based method, and the gray triangular dots from the PWE method. Obviously, no matter which method we use to calculate, there is no complete band gap for Al cylinders in a mercury host with the filling fraction $f = 0.4$. The frequency bands calculated by two methods are similar, but those from DtN-based method are lower than those from PWE method. That is to say, neglecting the transverse mode in solid sactterers will induce an higher estimate of the eigenfrequencies.

Phononics 2011: First International Conference on Phononic Crystals, Metamaterials and Optomechanics

Santa Fe, New Mexico, USA, May 29-June 2, 2011

PHONONICS-2011-0040

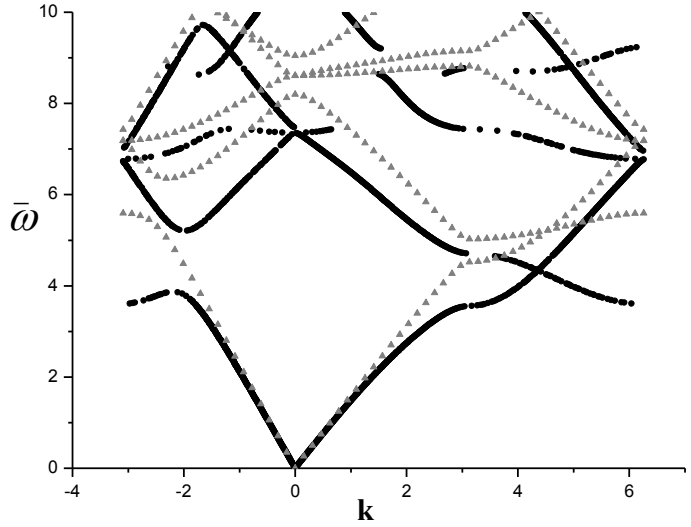

Figure 1 The dispersion curves of Al cylinders in mercury in a square lattice with $f = 0.4$. The black circular dots represent the band gaps from the DtN-based method, and the gray triangular dots from the PWE method.

References

[1] M. S. Kushwaha, P. Halevi, L. Dobrzynsi, and B. Diafari-Rouhani, Phys. Rev. Lett. **71**, 2022 (1993).
[2] M. S. Kushwaha, P. Halevi, G. Martinez, Phys. Rev. B. **49**, 2313 (1994).
[3] M. S. Kushwaha, P. Halevi, Appl. Phys. Lett. **64**, 1085 (1994).
[4] J. O. Vasseur, B. Djafari-Rouhani, L. Dobrzynsi, M. S. Kushwaha, and P. Halevi, J. Phys.: Condens. Matter **6**, 8759 (1994).
[5] M. S. Kushwaha, B. Djafari-Rouhani, J. Appl. Phys. **80**, 3191 (1996).
[6] M. S. Kushwaha, P. Halevi, J. Acoust. Soc. Am. **101**, 619 (1997).
[7] M. Kafesaki, and E. N. Economou. Phys. Rev. B, **60**, 11993 (1999).
[8] Z. Liu, C. T. Chan, and Ping Sheng, Phys. Rev. B. **62**, 2446 (2000).
[9] Y. Tanaka, Y. Tomoyasu, and S. Tamura. Phys. Rev. B, **62**, 7387 (2000).
[10] D. Garcia-Pablos, M. Sigalas, F. R. Montero de Espinosa, M. Torres, M. Kafesaki, and N. Garcia, Phys. Rev. Lett. **84**, 4349 (2000).
[11] D. Caballero, J. Sanchez-Dehesa, C. Rubio, R. Martinez-Sala, J. V. Sanchez-Perez, F. Meseguer, and J. Llinares, Phys. Rev. E. **60**, 6316 (1999).
[12] J. H. Yuan, and Y. Y. Lu. Opt. Soc. Am., **23**, 3217 (2006).

Phononics 2011: First International Conference on Phononic Crystals, Metamaterials and Optomechanics
Santa Fe, New Mexico, USA, May 29-June 2, 2011
PHONONICS-2011-0056

Negative refraction of elastic waves in 2D phononic crystals

Anne-Christine Hladky-Hennion[1], Charles Croënne[1], Bertrand Dubus[1], Jérôme Vasseur[1], Nichlas Swinteck[1, 2], Pierre A. Deymier[2] and Bruno Morvan[3]

[1] *Institut d'Électronique, de Microélectronique et de Nanotechnologie, UMR CNRS 8520, Cité Scientifique, 59652 Villeneuve d'Ascq Cedex, France,*
anne-christine.hladky@isen.fr, charles.croenne@isen.fr, bertrand.dubus@isen.fr, jerome.vasseur@univ-lille1.fr
[2] *Department of Materials Science and Engineering, University of Arizona, Tucson, Arizona 85721, USA*
swinteck@email.arizona.edu, deymier@email.arizona.edu,
[3] *Laboratoire Ondes et Milieux Complexes, FRE-3102 CNRS, Place Robert Schuman, 76610 Le Havre, France*
bruno.morvan@univ-lehavre.fr

Abstract: Negative refraction of elastic waves is evidenced in a two-dimensional phononic crystal (PC), made of a triangular lattice of steel rods embedded in epoxy. Experiments are carried out on a prism shaped PC inserted inside an epoxy block. The influence of different parameters is discussed in terms of image reconstruction.

Phononic crystals (PC's) may exhibit dispersion curves with a negative slope i.e. the wave vector and the group velocity vector associated with an acoustic wave point in opposite directions. This property is typical of a left handed material and implies a negative index of refraction in the Snell-Descartes law. Negative index PC's have the advantage of allowing the realization of flat super-lenses able to focus elastic waves with a resolution lower than the diffraction limit [1]. It has been shown that super-resolution can be achieved using a PC lens made of a triangular array of steel cylinders immersed in methanol and surrounded with water [2]. To go further for practical applications, it is more appropriate to consider a PC slab made with a solid matrix. In that case, longitudinal and transverse waves are coupled together in the PC, which makes the problem more complex.

In a recent paper, C. Croënne *et al* [3] have shown theoretically and experimentally the negative refraction of an elastic wave in a triangular array of steel rods in an epoxy block. The dispersion curves are presented in the first Brillouin zone and show that in the upper part, a branch with a negative slope is observed (Fig. 1). It corresponds to a mode with a predominantly longitudinal behavior. Moreover, the Equi-Frequency Contours (EFC), i.e. the intersection of the 3D dispersion curves with a horizontal plane, are circular: it means that the wavevector of the elastic wave and the group velocity are antiparallel, for any propagation direction (Fig. 2). As expected, the radius of the EFC clearly decreases as the frequency increases. Experiments have confirmed the theoretical simulations obtained using the finite element method. They are carried out on a prism shaped PC inserted inside an epoxy block. Measurement of the refraction angle at the output side of the PC shows the negative refraction of transverse or longitudinal waves through a solid PC. In the present paper, we analyze in details the elastic waves inducing a negative refraction. However, in the studied device, the refraction index of the PC is not matched with the refraction index of water, for immersed applications. Therefore, solutions are presented to match the refractive index of the PC with respect to the surrounding fluid. Finally, the occurrence of the focal spot is discussed (Fig. 3 and 4) and it is shown that many parameters are of interest in the construction of the focal spot: negative slope in the dispersion curve, the Equi Frequency Contours, index matching as well as impedance matching.

This work is supported by the Agence Nationale de la Recherche : ANR-08-BLAN-0101-01, SUPREME project.

Phononics 2011: First International Conference on Phononic Crystals, Metamaterials and Optomechanics
Santa Fe, New Mexico, USA, May 29-June 2, 2011
PHONONICS-2011-0056

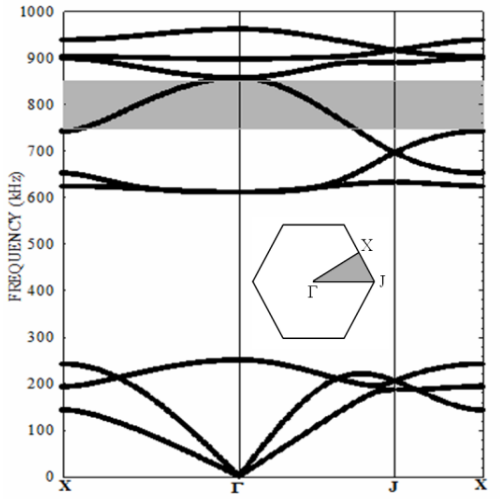

Figure 1: (a) Elastic band structure for the 2D PC made of a triangular array of steel rods in an epoxy matrix. The radius of the rods is 1 mm, the lattice parameter is 2.84 mm. In the frequency range [750 kHz, 860 kHz] (grey part) a negative branch is observed, corresponding to a mode with a predominantly longitudinal behaviour.

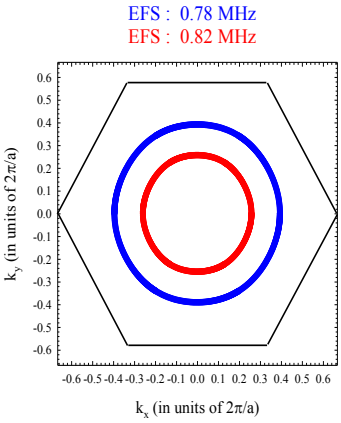

Figure 2: Equi Frequency Contours of the PC at 780 kHz (thick line) and 820 kHz (thin line).

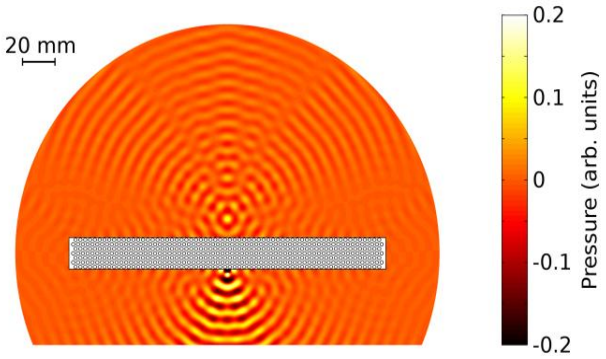

Figure 3: Simulated pressure field (normalized to a source amplitude of 1) for a PC-made flat lens immersed in a fluid, at 786 kHz. Fluid refractive index is matched to PC index. A point source is located below the lens, 3-mm away from the bottom interface. For clarity, the colorscale is cut to ±0.2 and thus some parts of the field map below the lens are out of colorscale (black/white regions). Losses are not taken into account.

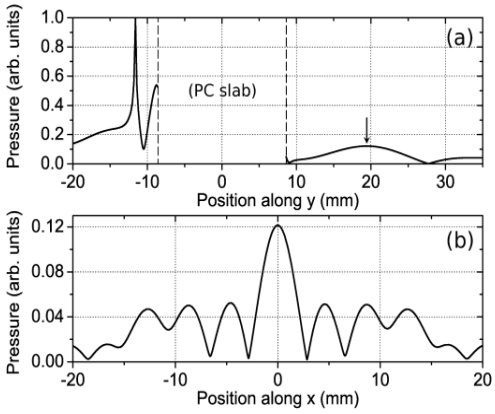

Figure 4: Plot of the pressure field amplitude (a) along the line perpendicular to the slab which includes the source point and (b) along the line parallel to the slab which includes the focal point, for the simulation of Fig. 3. Here the focal point is defined as the point of maximum amplitude on plot (a) (indicated by an arrow). On graph (a), the PC slab is situated between the two dashed lines

References

[1] A. Sukhovich, L.J. Jing, J.H. Page, Phys. Rev. B **77**, 014301 (2008).
[2] A. Sukhovich, B. Merheb, K. Muralidharan, J. O. Vasseur, Y. Pennec, P. A. Deymier and J. H. Page, Phys. Rev. Lett. **102**, 154301 (2009).
[3] C . Croënne, D. Manga, B. Morvan, A. Tinel, B. Dubus, J. Vasseur and A.-C. Hladky-Hennion, to be published in Phys. Rev. B, (2011).

Phononics 2011: First International Conference on Phononic Crystals, Metamaterials and Optomechanics
Santa Fe, New Mexico, USA, May 29-June 2, 2011
PHONONICS-2011-0059

Engineering of the Band gaps and transmissions in Phononic and phoxonic Crystal Slabs and Waveguides

B. Djafari Rouhani, C. Li, H. Larabi, Y. El Hassouani, Y. Pennec

Institut d'Electronique, de Microélectronique et de Nanotechnologies, UMR CNRS 8520, Université de Lille1, Avenue Poincaré, Cité Scientifique, 59652 Villeneuve d'Ascq, France
bahram.djafari-rouhani@univ-lille1.fr

Abstract: We report on our theoretical works about the engineering of band structures in phononic as well as dual phononic-photonic slabs and strips waveguides. Besides the conventional structure made of a periodic array of holes in a plate, we discuss the more recent geometry of pillars on a membrane or on a substrate. We discuss the best phoxonic structures displaying dual phononic-photonic band gaps and slow modes.

Following a great deal of works devoted to 2D phononic crystals [1] and their point and linear defects [2], the study of slabs of phononic crystals has become a topic of major interest during the last few years. Indeed, with an appropriate choice of their geometrical and physical parameters, these finite thickness structures can also exhibit absolute band gaps, similarly to the case of 2D structures. This makes them suitable to support the same confinement, guiding and filtering functionalities as in 2D phononic crystals, with the additional property of confinement in the vertical direction.

We have studied two types of phononic crystal slabs, namely the conventional case of a periodic array of holes in a plate such as silicon [3], and the new case of a periodic array of pillars on a membrane [4-7] (such as Si/SiO_2). We introduced the latter structure in 2008 especially because it can exhibit a low frequency gap, where the acoustic wavelength in any constituent material is several times larger than the period [4]. This gap is associated with a bending of the first three acoustic branches; its existence requires appropriate geometrical parameters, especially as concerns the thickness of the membrane and the height of the pillars whereas it remains robust against the choice of the constituting materials. One or more higher gaps can also appear in the band structure depending on the height of the pillars [4,5]. In particular, associated with the local resonances of the pillars, there are opening of gaps due to the bending of the acoustic branches (when they cut a local resonance) instead of their folding. Among different considered lattices, the triangular lattice provides better flexibility than the square and honeycomb lattices as concerns the choice of the geometrical parameters [5]. This is in contrast to the case of holes in a membrane where the honeycomb lattice provides the largest band gaps. When the thickness of the membrane increases, the absolute gap closes and one progressively recovers the case of pillars deposited on a semi-infinite substrate. Then, the band structure displays one or several surface localized branches below the bulk bands of the substrate.

We have studied the waveguiding phenomena in the above phononic crystals, especially in the case of pillars on a membrane [6]. Different types of linear defects are considered either by removing a row of pillars or by replacing in a row the materials or geometrical parameters of the pillars. In each case, we have made a detailed analysis of the confined modes, the transmitting or non-transmitting character of the corresponding bands, and the possibility of polarization conversion which could frequently occur.

Phonon transmission between two substrates connected by a periodic array of pillars has also been studied [7]. In particular, we have evidenced the existence of Fano resonances when a Perot-Fabry resonance inside a pillar falls in the vicinity of a zero of transmission; the latter results from the excitation by the normally incident wave of surface waves at the boundaries between the substrates and the pillars [7]. This and other features in the transmission spectrum, such as the regular oscillations associated with Fabry-Perot resonances inside the pillars or the existence of transmission gaps associated to the periodicity, are also discussed as a function of the geometrical and material parameters.

In a second part, we discuss the simultaneous existence of phononic and photonic band gaps in the above crystal slabs [5, 8], considering different lattices such as square triangular and honeycomb, as

Phononics 2011: First International Conference on Phononic Crystals, Metamaterials and Optomechanics
Santa Fe, New Mexico, USA, May 29-June 2, 2011
PHONONICS-2011-0059

well as the more general case of boron nitride (BN) lattices. With a periodic array of holes in a Si membrane [8], complete phoxonic band gaps can be obtained with the honeycomb lattice as well as with BN lattices close to honeycomb. Otherwise, all investigated structures present the possibility of a complete phononic gap together with a photonic gap of a given symmetry, either odd or even, depending on the geometrical parameters. With a periodic array of Si dots on a SiO_2 membrane [5], an appropriate choice of the geometrical parameters allows the existence of an absolute phoxonic gap. In contrast to the case of holes in a membrane, the more flexible lattice to keep the phononic gap open is now the triangular one, especially as concerns the thickness of the membrane. Moreover, this geometry allows the existence of the complete photonic gap over a wide range of parameters.
Let us mention a new idea [9] to create a complete photonic band gap by taking advantage of the anisotropy of the dielectric tensor (different refraction indices for the propagation of TE and TM modes).

Confined modes associated with defects such as waveguides and cavities in these structures will be useful for novel acousto-optic and sensing devices. In this work, we study the design of different waveguides that allow phononic and photonic dual guidance and confinement, especially with the possibility of single mode slow light and/or sound. Several structures are considered, among them one is obtained in a honeycomb lattice by cutting the crystal along the ΓK direction and by pushing the two half-crystals far from each other. In this way, the width of the waveguide can be taken as a parameter. Moreover, additional holes of different sizes are introduced on the sides of the waveguide.

As an alternative to the waveguides in a crystal slab, we also study 1D periodic waveguides constituted by making a nano-structuration in a suspended silicon strip waveguide One example is constituted by a 1D waveguide in which the sides are periodically rough. A similar case is obtained when periodical stubs are attached on both sides of the waveguide. We demonstrate the possibility of phononic and photonic dual band gaps in these structures and are investigating the designs of cavities that insure the confinement of both waves.

Finally, we would like to mention a calculation about the thermal transport in the frame of the above geometries. Namely, by using a lattice dynamic model, we have studied the directional thermal conductivity κ of a thin Si membrane covered by a 1D array of stretched Ge dots and discussed κ as a function of the angle of the heat flux with respect to the stretching direction [10].

Acknowledgments: This work was supported in part by the European Commission Seventh Framework Programs (FP7) under the FET-Open project TAILPHOX N° 233883 and IP project NANOPACK N° 216716.

References

[1] M.S. Kushwaha, P. Halevi, L. Dobrzynski and B. Djafari-Rouhani, *Phys. Rev. Lett.* **71,** 2022(1993); M.M. Sigalas and E.N. Economou, *Solid State Commun*. **86,** 141 (1993). For a recent review, see Y. Pennec, J.O. Vasseur, B. Djafari-Rouhani, L. Dobrzynski and P.A. Deymier, *Surf. Sci. Rep*.**65**, 229-291 (2010).
[2] A. Khelif, B. Djafari Rouhani, J.O. Vasseur and P.A. Deymier, *Phys. Rev.* B **68**, 024302 (2003); Y. Pennec, B. Djafari-Rouhani, J.O. Vasseur, H. Larabi, A. Khelif, A. Choujaa, S. Benchabane, and V. Laude, *Appl. Phys. Lett.* **87,** 261912 (2005).
[3] J.O. Vasseur, P.A. Deymier, B. Djafari-Rouhani, Y. Pennec and A.C. Hladky-Hennion, *Phys. Rev. B* **77,** 085415 (2008).
[4] Y. Pennec, B. Djafari-Rouhani, H. Larabi, J.O. Vasseur and A.C. Hladky-Hennion, *Phys. Rev. B* **78,** 104105 (2008).
[5] Y. El Hassouani, C. Li, Y. Pennec, E.H. El Boudouti, H. Larabi, A. Akjouj, O. Bou Matar, N. Papanikolaou, S. Benchabane, V. Laude, A. Martinez and B. Djafari-Rouhani, *Phys. Rev. B* **82,** 155405 (2010).
[6] Y. Pennec, B. Djafari-Rouhani, H. Larabi, A. Akjouj, J.N. Gillet, J. Vasseur and G. Thabet *Phys. Rev. B* **80,** 144302 (2009).
[7] Y. Pennec, B. Djafari-Rouhani and H. Larabi, Proc. SPIE, Vol. 7223 (Photonic and Phononic Crystal Materials and Devices IX), 72230F (2009). Ibidem *IUTAM Symposium on Recent Advances of Acoustic Waves in Solids*, Taipei, May 2009; Springer IUTAM Book Series, Volume 26, 2010, Edited by Tsung-Tsong Wu and Chien-Ching Ma, pages 127-138.
[8] Y. Pennec, B. Djafari Rouhani, E.H. El Boudouti, C. Li, Y. El Hassouani, J.O. Vasseur, N. Papanikolaou, S. Benchabane, V. Laude and A. Martinez, *Opt. Express*, **18**, 14301 (2010).
[9] D. Bria, M.B. Assouar, M. Oudich, Y. Pennec, J. Vasseur and B. Djafari Rouhani, *J. Appl. Phys*. (2011, under press).
[10] J.N. Gillet, B. Djafari Rouhani and Y. Pennec, Proceedings of Therminic 2009, Leuven, Belgium, October 2009, p. 203.

Phononics 2011: First International Conference on Phononic Crystals, Metamaterials and Optomechanics
Santa Fe, New Mexico, USA, May 29-June 2, 2011
PHONONICS-2011-0060

Surface/Interface Effects on Band Structures of Nano-sized Phononic Crystals

Ni Zhen[1], Yue-Sheng Wang[1], Ch. Zhang[2]

[1] *Institute of Engineering Mechanics ,Beijing Jiaotong University, Beijing 100044, China*
yswang@bjtu.edu.cn
[2] *Department of Civil Engineering, University of Siegen, D-57068 Siegen, Germany*
c.zhang@uni-siegen.de

Abstract: In this paper, the band structure of transverse waves propagating in a 2D phononic crystal composed of nanosized holes or elastic inclusions embedded in an elastic solid is calculated by using the method based on the Dirichlet-to-Neumann map. The Young-Laplace equation is applied to take into account of the surface/interface effects of the nanosized holes/inclusions. Detailed calculations are presented for the systems with or without the surface/interface effects. The results show that all bands descend with the first bandgap becoming lower and wider due to the existence of the surface/interface effects.

Introduction

Phononic crystals, due to their unique feature of band gap, exhibit potential applications in sound shielding, vibration isolation, design of new acoustic devices, etc., and therefore received considerable attention in the last decade.[1] With the rapid development of the communication technique, the size of acoustic devices is required to be smaller and smaller. For instance, the gigahertz communication generally requires the nanosized devices. In this case the influence of surface/interface energy and stress becomes significant.[2,3] It is expected that a phononic crystal should also exhibit unique physical properties when its lattice scale and scatterers' size are in the nanoscale.[4] Such nano phononic crystals will have potential application in design of nanostructure devices, nano electric-mechanical systems (NEMS), etc. In this paper, the wave propagation behaviors in nanosized phononic crystals will be studied by considering the surface/interface effects.

The method based on the Dirichlet-to-Neumann map[5] will be used to calculate the band structures. The method not only has advantages in accuracy, fast convergence and memory-saving but also can deal with the particular boundary conditions. This allows us to consider the surface/interface effects using the Young-Laplace equation.[6]

Problem statement and numerical method

The considered system is a 2D phononic crystal composed of circular holes or elastic inclusions in an elastic solid in a square lattice. The lattice constant, a, and the scatterers' radius, r_0, are all in nanoscales. Set the *z*-axis along and the *xy*-plane perpendicular to the axis of the scatterer. Then we consider a harmonic transverse wave polarized in the *z*-direction and propagating in the *xy*-plane. The governing equation of this purely transverse harmonic wave is $\nabla^2 w + k^2 w = 0$ where w is the displacement component in *z*-direction with the time harmonic factor $e^{-i\omega t}$ suppressed; and $k = c_t / \omega$ are the wave number with c_t being the transverse wave velocity and ω the angular frequency.

To taking into account of the surface/interface effects, we impose the following famous Young-Laplace equation[6] on the surface/ionterface of the hole/inclusion:

$$[\sigma_{rz}] = -\frac{1}{r_0}\frac{\partial \sigma^s_{\theta z}}{\partial \theta},\ \sigma^s_{\theta z} = 2\left(\mu^s - \tau_0\right)\varepsilon^s_{\theta z}, \tag{1}$$

where $\sigma^s_{\theta z}$, $\varepsilon^s_{\theta z}$, μ^s are the surface stress, strain and modulus; τ_0 is the residual stress (generally we take $\tau_0 = 0$); and $[\sigma_{rz}]$ represents the difference between the bulk stresses of the matrix and scatterer.

The method based on the Dirichlet-to-Neumann map (DtN map) will be used to calculate the band structures of the nanosized phononic crystals with consideration of surface/interface effects. The

Phononics 2011: First International Conference on Phononic Crystals, Metamaterials and Optomechanics
Santa Fe, New Mexico, USA, May 29-June 2, 2011
PHONONICS-2011-0060

method was first developed by Yuan and Lu[5] for calculating the band structures of photonic crystals. It can be extended to the phononic crystals in a straight forward manner when the purely transverse wave is considered. The key steps of the method are: (*i*) represent the general solution of the wave equations by the cylindrical wave expansions with coefficients being determined by using the Young-Laplace equation at the surface/interface; (*ii*) obtain the DtN map, which relates the displacement component with its normal derivation on the boundary of the square unit cell based on the general solution (For the purpose of numerical computation, the discrete form of the DtN map should be given. To this end, we select N points on each edge of the square unit cell and write the DtN map in a $4N\times4N$ matrix); (*iii*) then apply the Bloch theorem and the periodicity conditions to the boundaries of the unit cell, and formulate the problem in an eigenvalue equation; (*iv*) finally solve the eigenvalue equation to obtain the dispersion relation, i.e. the band structures.

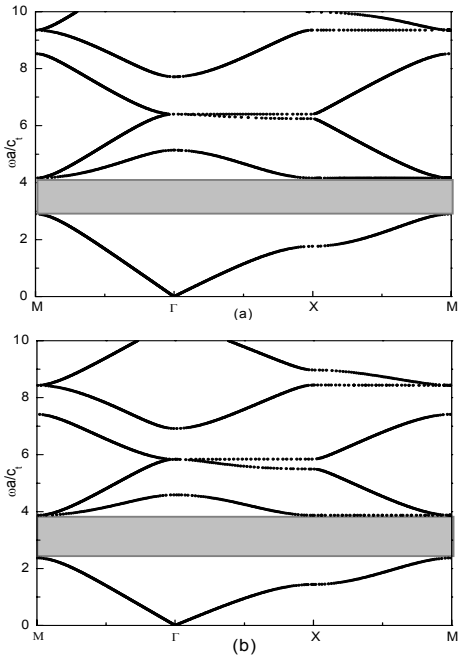

Figure 1 The band structures of the phononic crystal with a square lattice of vacuum cylindrical holes in an aluminum host with the filling fraction of 0.55: (a) neglecting the surface effect; (b) taking into account of the surface effect, $(\mu^s-\tau_0)/\mu_{\text{matrix}}r_0$=–0.06.

Results and Discussion

Two systems are computed by using the DtN-based method. One is a square lattice of vacuum cylindrical holes in an aluminum host; another is a square lattice of aluminum cylinders in a tungsten host. The band structures for these two systems with and without the surface/interface effects are presented in Figs. 1 and 2.

The results show that, due to the existence of the surface/interface effects, all bands descend and the first band gap becomes lower and a little wider. Further calculations show that the position of the band gap decreases with a very slight increase of the width as the absolute value of the parameter $(\mu^s-\tau_0)/\mu_{\text{matrix}}r_0$ increases.

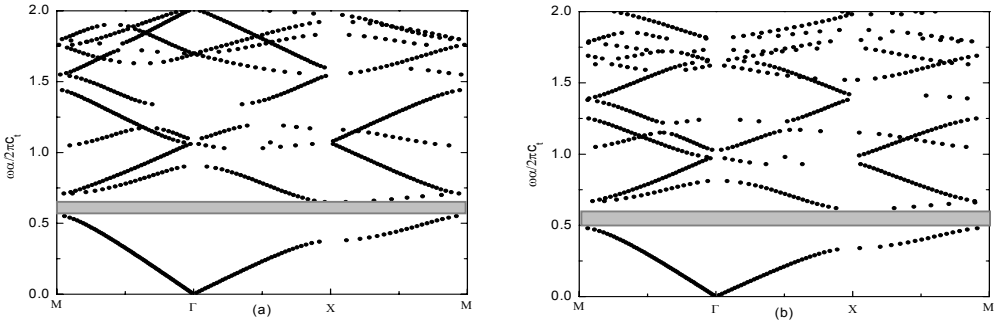

Figure 2 The band structures of the phononic crystal with a square lattice of aluminum cylinders in a tungsten host with the filling fraction of 0.55: (a) neglecting the interface effect; (b) taking into account of the interface effect, $(\mu^s-\tau_0)/\mu_{\text{matrix}}r_0$=–0.06.

References

[1] Y. Pennec, B. Djafari-Rouhani, H. Larabi, J. Vasseur, and A. –C. Hladky-Hennion, *Phys. Status Solidi C* **6**, 2080-2085 (2009).
[2] R. E. Miller, and V. B. Shenoy, *Nanotechnology* **11**, 139-147(2000).
[3] S. M. Hasheminejad, and R. Avazmohammadi. *Comp. Sci. Tech*. **69**, 2538-2546(2009).
[4] N. Gomopoulos, D. Maschke, C. Y. Koh, E. L. Thomas, W. Tremel, H. -J. Butt, and G. Fytas, *Nano Lett.* **10**, 980-984(2010).
[5] J. H. Yuan, and Y. Y. Lu, *Opt. Soc. Am*. **23**, 3217-3222(2006).
[6] M. E. Gurtin, and A. I. Murdoch, *Arch. Ration. Mech. Anal.*, **57**, 291-323(1975).

Phononics 2011: First International Conference on Phononic Crystals, Metamaterials and Optomechanics
Santa Fe, New Mexico, USA, May 29-June 2, 2011
PHONONICS-2011-0061

Phononic Crystal Sensors

M. M. Sigalas, N. Aravantinos-Zafiris

Department of Materials Science, University of Patras, 26504 Patras, Greece,
sigalas@upatras.gr, naravadinos@upatras.gr

Abstract: Numerical studies of phononic crystals for sensors applications are presented. The sensitivities of the structures on their parameters are studied. Particular attention was given in structures that can be probed with both electromagnetic and elastic waves.

Phononic materials are computationally studied using the finite difference time domain (FDTD) method for possible applications as sensors. The structures studied where similar with the ones used in photonic crystal sensors applications.[1] They are structures with air holes and that allows the detectable materials to be more accessible in the structure. Consequently, the changes in the frequency response of elastic waves propagating in those structures are higher.

The first structure studied was an epoxy slab with a square lattice of air holes. The lattice constant is 333nm, the radius of the air holes is 100nm and the thickness of the slab is 333nm. The transmission of elastic waves propagating through this structure shows a gap at around 6 GHz (solid line in Fig. 1). Covering the surface of this structure with a 16.6nm thick layer of water (see dash line in Fig. 1) changes the upper and lower band gap edges. Therefore it can be used a sensor for detecting different materials such as moisture and liquids or even proteins and other biological molecules.

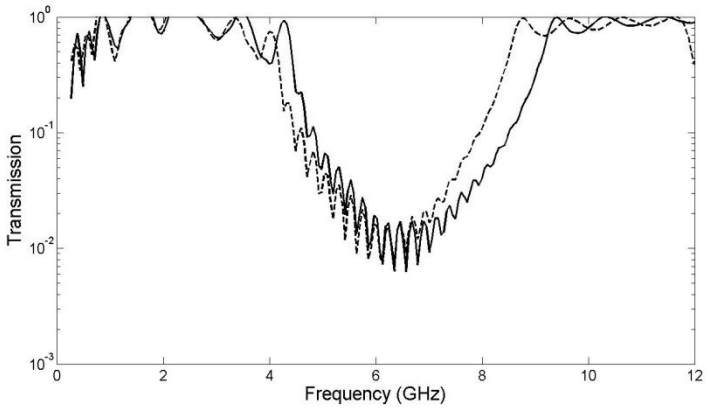

Figure 1 The transmission spectrum of elastic waves in an epoxy slab with a square lattice of air holes.

The second structure studied is a three dimensional structure consisting of alternate layers of air rods perpendicular to each other. This is the so called layer by layer structure.[2] The background material is silicon. The separation of the rods in each layer is 1000nm, the width of the rods 500nm and the thickness of each layer is 333.3nm. A band gap appears at around 1.2 GHz (see solid line in Fig. 2). Covering the surface of the air rods with a 33.3nm layer of water, the response of elastic waves propagating through the structure changes (see dash line in Fig. 2).

Phononics 2011: First International Conference on Phononic Crystals, Metamaterials and Optomechanics

Santa Fe, New Mexico, USA, May 29-June 2, 2011

PHONONICS-2011-0061

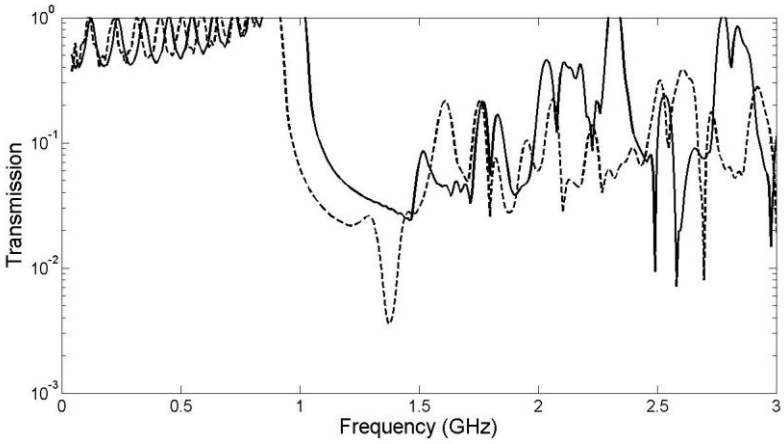

Figure 2 The transmission spectrum of elastic waves in a layer by layer structure made of air holes in silicon.

The different parameters affecting the sensitivity of these structures will be presented, such as the size of the holes and the thickness of the slab. Results for defect structures will be presented. Also, the possibility of using those structures as hybrid sensors that can be probed with both electromagnetic and elastic waves will be discussed.

References

1. E. Chow, et. al., Opt. Lett. 29, 1093 (2004); S. Zlatanovic, et. al., Sensors Actuators B 141, 13 (2009).
2. K. M. Ho, et. al, Solid State Commun. 89, 413 (1994).

Phononics 2011: First International Conference on Phononic Crystals, Metamaterials and Optomechanics
Santa Fe, New Mexico, USA, May 29-June 2, 2011
PHONONICS-2011-0065

Liquid Sensor Utilizing Phononic Crystals

Ralf Lucklum[1] , Mikhail Zubtsov[1], Manzhu Ke[1,2]

[1] *Institute of Micro and Sensor Systems, Otto-von-Guericke-University, Magdeburg, Germany*
ralf.lucklum@ovgu.de, mikhail.zubtsov@ovgu.de
[2] *Department of Physics, Wuhan University, China*
mzke@whu.edu.cn

Abstract: A phononic crystal device is investigated as a sensor platform combining bandgap engineering with resonant transmission. We compare several approaches: a one-dimensional arrangement with a thin liquid analyte layer, two-dimensional phononic crystals with and without symmetry reduction and incidence directions normal and perpendicular to the plate.

Motivation:

Ultrasonic sensors and acoustic microsensors have been successfully exploited as chemical sensors for liquids. Ultrasonic sensors first of all use the dependence of speed of sound on the composition of a liquid mixture whereas acoustic microsensors achieve chemical sensitivity with a specific coating. Time-of-flight and resonance frequency, respectively, are the most utilized measurement parameters. Both principles cannot be combined with microfluidic systems without severe limitations. The demand on sensors is permanently increasing which provide data related to material properties like concentration of an analyte in a fluid, conversion rate in a microreactor or adsorption of biomolecules. Phononic crystals have the capability to closing this gap since characteristic dimensions can be scaled in an appropriate range without losing its most pronounced feature, the acoustic band gap.

Sensor Scheme:

Phononic crystals are periodic composite materials with spatial modulation of acoustically relevant parameters like elasticity, mass density and longitudinal and transverse velocities of elastic waves. When applied as sensor, the material of interest constitutes one component of the phononic crystal, e.g., a fluid in the holes of a phononic crystal with a solid matrix. If the value of interest, let's say the concentration of a contaminant in a liquid mixture, changes acoustic properties of this mixture, the acoustic properties of the phononic crystal will also change. Transmission or reflection coefficients are appropriate parameters for measurement and used to localize a characteristic feature of the phononic crystal. For a sensor application, a transmission peak within the band gap or a transmission dip outside the band gap is the most favorable feature since the respective frequency of maximum/minimum transmission is easy to determine. The sensor scheme therefore relies on the determination of the frequency dependence of maximum/minimum transmission on the physical or chemical value of interest.

Sensitivity:

The sensitivity of the sensor, S_f can be defined as the ratio of frequency shift, Δf, and change of the input parameter, Δx:

$$S_f = \frac{\Delta f}{\Delta x} \tag{1}$$

The sensitivity has been found to be dependent on the probing frequency, f_0. Furthermore, in terms of the detection limit the peak half band width, f_{HBW}, must be considered, hence the reduced sensitivity, S_{fr}, gives much better insights to the sensor capabilities:

$$S_f = \frac{\Delta f}{\Delta x f_0 \Delta f_{HBW}} \tag{2}$$

Phononics 2011: First International Conference on Phononic Crystals, Metamaterials and Optomechanics
Santa Fe, New Mexico, USA, May 29-June 2, 2011
PHONONICS-2011-0065

Sensor Realizations:

The simplest realization of a sensor is the parallel arrangement of several layers of metal plates and a liquid in between. The transmission properties can by analytically calculated; the results can serve as proof-of-principle. Furthermore, relations relevant for a sensor application could be revealed. It is possible to realize geometries with well-defined transmission peaks in the band gap. The number of peaks increases with the number of layers, whereas breaking symmetry reduces the number of peaks. The sensitivity related to those peaks is different and in the order of macroscopic sensors. Peaks could be found which are independent of liquid properties; they may act as reference. The peak half band width decreases with the number of layers. Experiments have been performed at frequencies around 1 MHz, requiring mm dimensions.

Sensors utilizing 2D phononic crystal have been studied in two basic arrangements, with in-plane excitation and detection of waves and an incidence direction perpendicular to the plate. For comparison reasons, the design has been optimized for similar probing frequencies. In both realizations a liquid fills all holes of the phononic crystal plate; in the latter case it also covers both surfaces. In the 'classical' arrangement a design with a band gap between 1.2 MHz and 1.9 MHz could be found which moves when a liquid with different properties is applied. More importantly, a specific peak could be identified which represents changes in liquid properties. However, an unfavorable large number of peaks appears in the band gap when the phononic crystal holes are liquid filled. To reduce the number of peaks and improve the separation the symmetry of the lattice has been reduced by stretching and distorting. The reduced sensitivity achieved so far is similar to the one-dimensional case and indicates similar physical background for the appearance of these narrow transmission windows. They are basically supported by resonance-like phenomena. From the sensor point of view the respective vibration modes are of superior importance since it allows distinguishing between volume and surface/interfacial effects. Detail about simulation tools are given in [1].

When applying normal incidence of waves, also a characteristic transmission peak, see Fig. 1, could be found which strongly depends on liquid sound velocity. Again, this extraordinary transmission feature is supported by resonance phenomena in the phononic crystal structure. The half band width of this peak is larger; hence the reduced sensitivity is lower than in the other realizations. On the other hand, the effect is more robust and the insertion loss of the device is much lower, an important issue from a practical point of view. Since the peak frequency position is completely defined by material properties of the participating materials and geometry (hole radius and lattice constant) no calibration is needed. We therefore could also analyze sytematic error propagation. This analysis could, for example, clarify systematic differences between theory and experiment. Details will be given in [2].

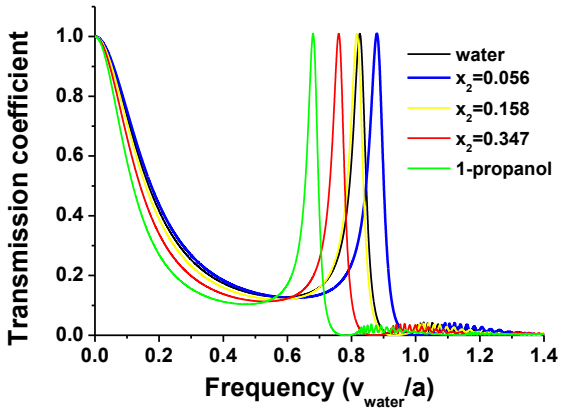

Figure 1 Results of FDTD calculations of the transmission spectrum of ultrasonic waves through a 2D phononic crystal at normal incidence. The phononic crystal consists of a steel plate with square lattice of holes. The composition of the liquid gradually changes from pure water (black) to pure propanol (green). The shift of the maximum transmission peak frequency reflects the extreme in speed of sound having the highest resonance frequency at molar ratio $x_2 = 0.056$.

References

[1] M. Zubtsov, R. Grundmann, R. Lucklum, subm. to Phononics 2011.
[2] M. Ke, M. Zubtsov, R. Lucklum, subm. to Phononics 2011.

Phononics 2011: First International Conference on Phononic Crystals, Metamaterials and Optomechanics
Santa Fe, New Mexico, USA, May 29-June 2, 2011
PHONONICS-2011-0072

Propagation and Transmission of Elastic SH-Waves in Functionally Graded Phononic Crystals

Mikhail V. Golub[1], Sergey I. Fomenko[1], Tinh Quoc Bui[2], Chuanzeng Zhang[2]

[1] *Institute for Mathematics, Mechanics and Informatics, Kuban State University, Stavropolskaya Str. 149, 350040 Krasnodar, Russian Federation*
m_golub@inbox.ru; sfom@yandex.ru;
[2] *Department of Civil Engineering, University of Siegen, D-57068 Siegen, Germany*
tinh.buiquoc@gmail.com; c.zhang@uni-siegen.de;

Abstract: The boundary value problem of elastic SH-wave propagation in one-dimensional phononic crystals composed of functionally graded interlayers arisen from the solid diffusion of homogeneous isotropic material of the crystal is considered. The localization phenomena, transmission and band gaps due to the material gradation are investigated.

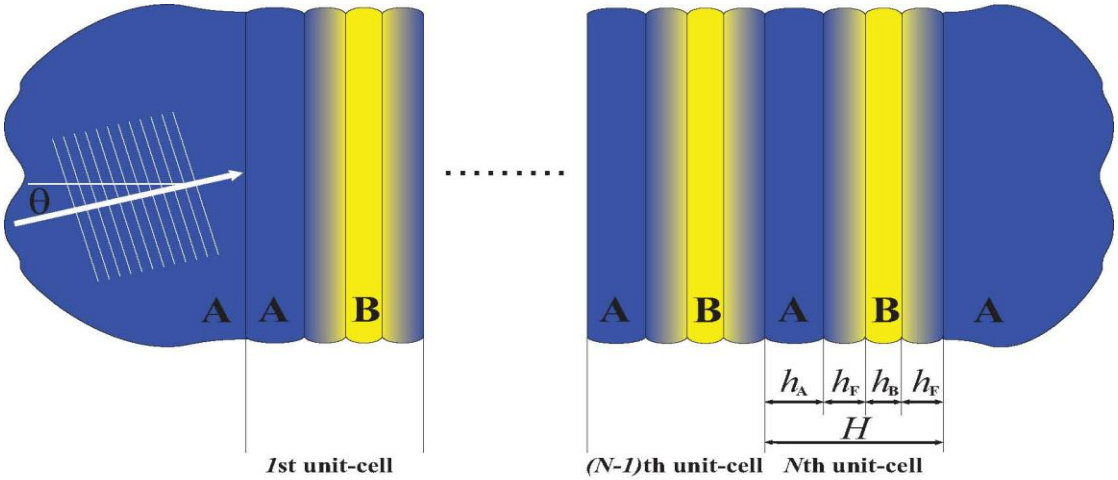

Figure 1 Geometry of the problem: periodic composite of functionally graded unit-cells.

The present work aims to propose a detailed study to band-structure analysis and elastic wave propagation in one-dimensional phononic crystals of functionally graded materials (FGM) by using the boundary integral equation method and an extended transfer matrix method. The structure of the phononic crystals is composed of finite periodically spaced unit-cells in one-dimension made of both functionally graded and isotropic materials (Figure 1). The power and exponential laws representing the material properties of the FGM are used. In both cases two approaches are used, namely, approximate modeling of the FGM structure by a certain number of isotropic layers and exact solution of the boundary value problem (Figure 2).

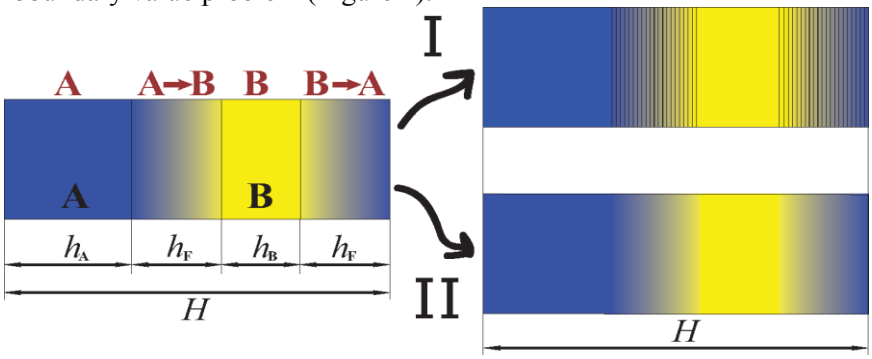

Figure 2 Models used for the simulation of functionally graded unit-cells (isotropic layers or exact solution).

Typical phenomena involving wave localization and transmission are analyzed, and the possibility of the damaged layers introduced following reference[1] is discussed. The comparison of the band gaps calculated using the present approaches as a special case of one-dimensional (1D) phononic crystal for SH propagation with that of FGM rod[2] is successfully carried out. This illustrates the applicability and the accuracy of the pro-

Phononics 2011: First International Conference on Phononic Crystals, Metamaterials and Optomechanics
Santa Fe, New Mexico, USA, May 29-June 2, 2011
PHONONICS-2011-0072

posed methods compared with the existing reference solutions. The model can be extended to other types of waves (P-SV waves) and cases with different types of internal inhomogeneities (cracks, imperfect bonding etc.).

The plane SH-wave in an elastic media is governed by the following equation

$$\frac{\partial}{\partial z}\left(\mu(z)\frac{\partial u(x,z,t)}{\partial z}\right)+\mu(z)\frac{\partial^2 u(x,z,t)}{\partial x^2}=\rho(z)\frac{\partial^2 u(x,z,t)}{\partial t^2} \tag{1}$$

Here $\rho(z)$ and $\mu(z)$ are the mass density and the shear modulus of the periodic layered structure. The material constants in the homogenous layers A and B of the unit-cell are continuously varied through a diffusion layer between A and B (Figure 1). The displacement $u(z)$ and stress $\tau(z)=\mu\,\partial u/\partial z$ fields are continuous at the interfaces of the layered structure.

The transfer matrix method for phononic crystals with FGM sublayers can be modified in the following way. Let us consider the j-th layer of the unit-cell bounded by the $z=z_j^{(1)}$ and $z=z_j^{(2)}$ planes. From the governing equation (1) the generalized displacement and stress state vector $\mathbf{v}=\{u,\tau\}$ is expressed in terms of the T-matrix [3,4]

$$\mathbf{v}(z)=\mathbf{T}_j(z-z_j^{(1)})\mathbf{v}_j^{(1)},\qquad z\in[z_j^{(1)},z_j^{(2)}],$$

where $\mathbf{v}_j^{(1)}$ is the incoming wave field, $\mathbf{T}_j$ is the T-matrix (transfer matrix) that is expressed in term of the fundamental solutions $\mathbf{v}_{j1}=\{u_{j1},\tau_{j1}\}$ and $\mathbf{v}_{j2}=\{u_{j2},\tau_{j2}\}$

$$\mathbf{T}_j(z)=\begin{pmatrix}u_{j1} & u_{j2}\\ \tau_{j1} & \tau_{j2}\end{pmatrix}$$

Here $\mathbf{v}_{j1}$ and $\mathbf{v}_{j2}$ are solutions of the following boundary value problems

$$\frac{d\mathbf{v}_{jk}}{dz}=\mathbf{B}(z+z_j^{(1)})\mathbf{v}_{jk},\quad \mathbf{v}_{j1}\big|_{z=0}=\{1,0\},\ \mathbf{v}_{j2}\big|_{z=0}=\{0,1\};\ \mathbf{B}(z)=\begin{pmatrix}0 & 1/\mu\\ -\mu q^2 & 0\end{pmatrix} \tag{2}$$

The T-matrix of a homogenous layer (A or B) is represented by an explicit formula (see e.g. reference[5]). Except the particular cases (e.g., exponential law) the T-matrix of the FGM layer is evaluated numerically. The numerical solution of the boundary value problem (2) is an explicit approach to be developed following reference[6]. Both models (see Figure 2) for the problem are compared with respect to their efficiency and accuracy. The convergence of both approaches, the band gaps and the transmission coefficients for different material gradation laws are investigated by numerical examples.

The work is supported by the Ministry of Education and Science of Russian Federation (Project 1.1.2/10463), the German Research Foundation (DFG, Project No. ZH 15/11-1) and the German Academic Exchange Service DAAD, which are gratefully acknowledged.

References

[1] J. Baik, R. Thompson, *Journal of Nondestructive Evaluation*, **4**, 177-196 (1984).
[2] M.-L. Wu, L.-Y. Wu, W.-P. Yang, L.-W. Chen, *Smart Materials and Structures* **18**, 115013 (2009).
[3] M. Born, E. Wolf, *Principles of Optics: Electromagnetic Theory of Propagation, Interference and Diffraction of Light*. Oxford, Pergamon Press (1964).
[4] O. Matsudaa, Ch. Glorieux, *Journal of Acoustical Society of America* **121 (6)**, 3437-3445 (2007).
[5] F.-M. Li, Y.-S. Wang, *International Journal of Solids and Structures* **42**, 6457-6474 (2005).
[6] E.V. Glushkov, N.V. Glushkova, *Journal of Computational Acoustics*, **9(3)**, 889-898 (2001).

Phononics 2011: First International Conference on Phononic Crystals, Metamaterials and Optomechanics
Santa Fe, New Mexico, USA, May 29-June 2, 2011
PHONONICS-2011-0073

Phononic crystals with complete phase space properties

P.A. Deymier[1], N. Swinteck[1], S. Bringuier[1], K. Muralidharan[1], J.O. Vasseur[2], J-F. Robillard[2], A.-C. Hladky-Hennion[2], A. Sukhovich[3] and J.H. Page[3]

[1] *Department of Materials Science and Engineering, University of Arizona, Tucson, Arizona 85721, USA,* deymier@email.arizona.edu, swinteck@email.arizona.edu, stefanb@email.arizona.edu, Krishna@email.arizona.edu

[2] *Institut d'Électronique, de Microélectronique et de Nanotechnologie, UMR CNRS 8520, Cité Scientifique, 59652 Villeneuve d'Ascq Cedex, France,* jerome.vasseur@univ-lille1.fr, jean-francois.robillard@isen.fr, anne-christine.hladky@isen.fr,

[3] *Department of Physics and Astronomy, University of Manitoba, Winnipeg, Manitoba, R37 2N2, Canada* jhpage@cc.umanitoba.ca, alexey.sukhovich@geoazur.obs-vlfr.fr

Abstract: We review and demonstrate properties of phononic crystals over their complete phase space, namely, spectral (ω-space), wave vector (*k*-space) and phase (*φ*-space) properties. The later two properties are applied to acoustic imaging with a phononic crystal flat lens and to interference-driven acoustic Boolean logic.

Phononic crystals (PC) are composite materials which derive their spectral (ω-space) and wave vector (*k*-space) properties from the scattering of elastic waves by periodic arrays of elastic inclusions embedded in an elastic matrix. Perfect PCs and ones with defects have been shown to exhibit numerous useful spectral capabilities including transmission band gaps, local modes for guiding, filtering and multiplexing [1]. *k*-space properties result from features in the band structure that impact refraction. Phase (*φ*-space) properties can result from non-collinear wave and group velocity vectors in the PC as well as the degree of refraction [2]. PC may show negative refraction leading to the possibility of developing flat lenses for focusing acoustic waves. To illustrate *k*-space functionalities, we discuss acoustic wave focusing (resulting from negative refraction) and subwavelength imaging capabilities of a PC flat lens consisting of a triangular array of steel cylinders in methanol, all surrounded by water (Fig. 1). The image resolution of the PC flat lens beats the Rayleigh diffraction limit because bound modes in the lens can be excited by evanescent waves emitted by the source. These are modes that only propagate in the direction parallel to the water/lens interface. These modes resonantly amplify evanescent waves that contribute to the reconstruction of an image. By employing a combination of experimental and computational (Finite Difference Time Domain (FDTD)) methods, we explore the effect on the image resolution and focal point on various structural and operational parameters such as source frequency, geometry of the lens, source position and time. The mechanisms by which these factors affect resolution are discussed in terms of the competition between the contribution of propagative modes to focusing and the ability of the source to excite bound modes of the PC lens.

We also demonstrate that the band structure of a two-dimensional PC constituted of a square array of cylindrical Polyvinylchloride (PVC) inclusions in an air matrix can be used to control the relative phase of acoustic waves. Phase control is due to the propagation of acoustic waves in the PC with wave vectors that are not collinear with their group velocity vectors. This condition implies that excited Bloch waves travel at different phase velocities in the direction of their group velocity. By modulating the phase between waves in the PC, destructive or constructive interference can occur and through this information can be encoded. In addition to phase control between pairs of acoustic beams, the band structure of this PC allows for superposition of wave vectors via the excitation of the same Bloch modes. This unique feature once again permits the possibility of destructive or constructive interferences within the PC; therefore it is another mechanism in which information can be encoded through relative phase. These two schemes of encoding information in phase establish the Boolean logic necessary for gating functions. The realization of the NAND and XOR gates (fig. 1) was demonstrated through FDTD technique. There are also operating frequencies for which the circular equi-frequency contour (EFC) in air is larger than the first Bril-

Phononics 2011: First International Conference on Phononic Crystals, Metamaterials and Optomechanics
Santa Fe, New Mexico, USA, May 29-June 2, 2011
PHONONICS-2011-0073

louin zone of the PC, allowing several Bloch modes to exit the crystal, leading to the phenomenon of beam splitting. This PC illustrates the possibility of extending the range of functionalities from spectral and wave vector properties to phase (φ-space) properties.

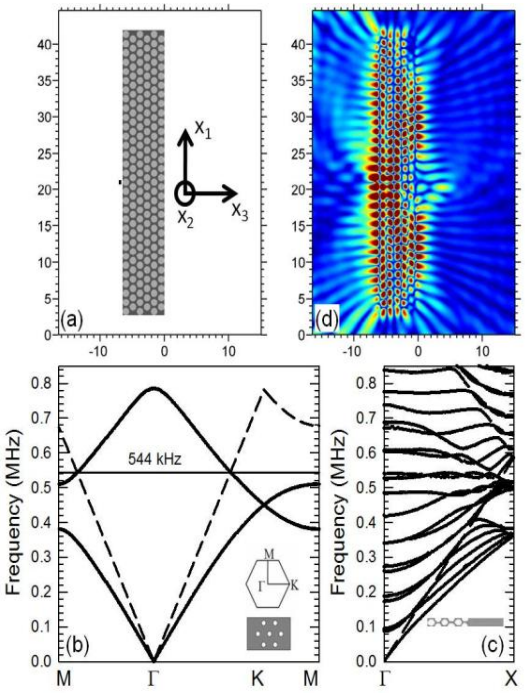

Figure 1: (a) Phononic Crystal system consisting of a triangular lattice of steel cylinders (light grey) in a methanol matrix (dark grey), all surrounded by water (white). The short thick line located close to the center of the left side of the crystal represents the sound source. (b) FDTD dispersion curves of the infinite crystal (solid lines). The dashed line represents the dispersion curve in water. The intersection of the water cone with a negative group velocity band determines the frequency that results in a negative effective index of -1 for the PC. The inset shows the triangular crystal lattice of the PC with the corresponding unit cell and the contour of the first Brillouin zone. (c) FDTD band structure in the ΓX direction (parallel to the surface) for a finite 6-layer crystal. Modes above water line correspond to propagating modes, while those which fall below are modes bound to the PC slab, which exhibit evanescent character. The inset depicts the supercell used in the calculation. (d) FDTD calculation of the average of the absolute value of the pressure over one period. On the exiting (right) side of the PC, an image is formed in the center accompanied by pressure lobes that decrease in magnitude as the distance from the surface of the crystal increases.

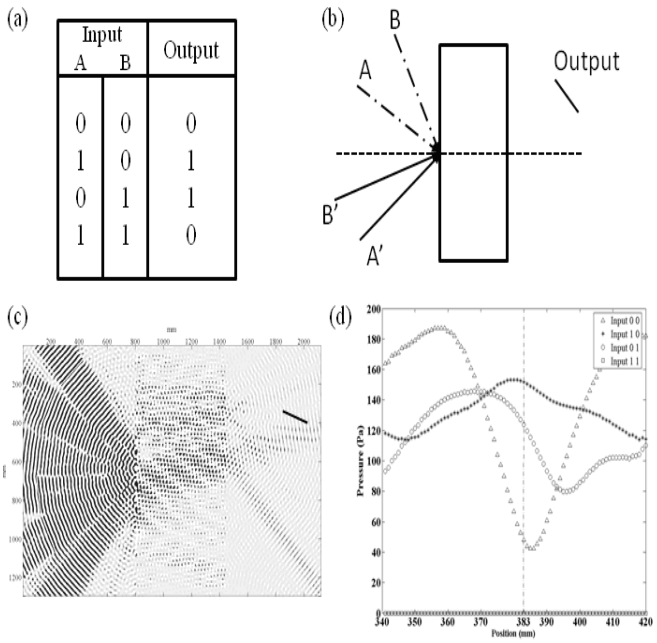

Figure 2: (a) Truth table for XOR logic gate. (b) schematic of PC logic gate, A' and B' are constant amplitude sources which are in phase. A and B are amplitude modulated sources which are out of phase with respect to A' and B'. (c) FDTD results for input (1 1) with output (0), black line represents where pressure detector is placed. (d) Average pressure cuts of all input cases. Pressure value for input (0 0) at 383mm is taken to be the pressure threshold.

References

[1] Yan Pennec, Jérôme O. Vasseur, Bahram Djafari-Rouhani, Léonard Dobrzynski, Pierre A. Deymier, Surf. Sci. Reports **65**, 229 (2010).
[2] A. Sukhovich, B. Merheb, K. Muralidharan, J.O. Vasseur, Y. Pennec, P.A. Deymier, J.H. Page, Physical Review Letters **102**, 154301 (2009)

Phononics 2011: First International Conference on Phononic Crystals, Metamaterials and Optomechanics
Santa Fe, New Mexico, USA, May 29-June 2, 2011
PHONONICS-2011-0082

Propagation of the Elastic Wave in One-dimensional Randomly Disordered Solid-liquid Phononic Crystals

A L Chen[1] , Y S Wang[2], C Zhang[3]

[12] Institute of Engineering Mechanics, Beijing Jiaotong University, Beijing 100044, China, alchen@bjtu.edu.cn, yswang@bjtu.edu.cn
[3] Department of Civil Engineering, University of Siegen, D-57068 Siegen, Germany c.zhang@uni-siegen.de

Abstract: The wave propagation and localization in one-dimensional (1D) randomly disordered solid-liquid phononic crystals are studied in this paper. The transfer matrix method is used to calculate the localization factor which is introduced to describe the band structures for the disordered phononic crystals. The fluid-structure interaction is considered and the oblique incidence is studied.

Introduction

Since Kushwaha[1] proposed the concept of the phononic crystal (PNC) in 1993, an artificial periodic elastic/acoustic structure that exhibits so-called "phononic band gaps", a lot of results on the mechanism and the tuning of band gaps for various systems as well as the defect states of the systems with point or line defects have been reported, cf. the website http://www.phys.uoa.gr/phononics/. When a point, line or surface defect is introduced into an ordered PNC, waves will be localized near the defects[2]. This property can be used to design new acoustic wave devices such as wave filters, waveguides, resonators, et al. PNCs mentioned above are strictly periodic in which all waves are extended states or have little defects in which some waves are localized states but most waves are extended states, so the Bloch theorem can be used[3]. Random disorder, caused by randomly distributed material defaults or manufacture errors during production process, is a different case. It is well known that the presence of the disorders may lead to localization phenomenon like the well-known Anderson localization of electron waves in disordered lattices[4]. Researches on randomly disordered PNCs are limited. In this paper we will study the acoustic waves propagating in the one-dimensional (1D) randomly disordered solid-liquid PNC. The general case of wave propagation in an arbitrary direction will be considered. The transfer matrix method[5] will be employed by considering the coupling conditions of the solid and liquid media at the interface. Instead of calculating the transmitted waves, we will use a well-defined localization factor to characterize the band structures and localization phenomenon of the system.

The Method

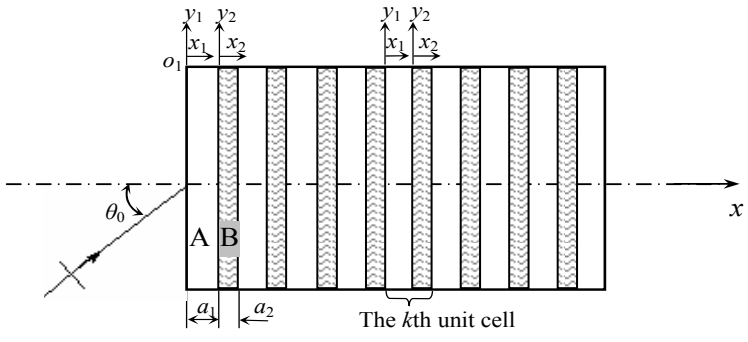

Figure 1 Schematic diagram of a 1D phononic crystal

Consider a 1D PNC shown in Fig.1. The PNC consists of n unit cells. Each unit cell includes two subcells made by two different materials (the solid material A and the liquid material B) and denoted by subscript j =1,2. In this paper the transfer matrix method is used. As we know, the transfer matrix is 2×2 and 4×4 for the liquid and solid layer, respectively. Considering the fluid-structure interaction condition the 4×4 transfer matrix for the solid layer can be deduced to the 2×2 matrix.

The solutions to the equations of wave motion are obtained by introducing potential functions to those equations. The transfer matrix between two consecutive sub-layers is obtained according to conditions

Phononics 2011: First International Conference on Phononic Crystals, Metamaterials and Optomechanics
Santa Fe, New Mexico, USA, May 29-June 2, 2011
PHONONICS-2011-0082

at the interface between the solid and fluid. The localization factor γ of the 1D PNCs is calculated by the transfer matrix method. The formulate of the localization factor is given as[6]

$$\gamma_m = \lim_{n\to\infty} \frac{1}{n} \sum_{k=1}^{n} \ln \left\| \hat{\boldsymbol{\nu}}_{2R,m}^{(k+1)} \right\| \tag{1}$$

When the localization factors in the figures are equal to zero then the according frequency intervals are known as pass bands. When the localization factors are bigger than zero then the intervals are known as band gaps.

Numerical Examples and Discussions

We consider the PNC composed of Al (material A) and Water (material B). The disordered parameter is the thinkness of the liquid layer (a_2) which can be expressed as $a_2 = \overline{a}_2[1+\sqrt{3}\delta(2t-1)]$ where $t \in (0,1)$ is a random variable; and δ is the disordered degree. It is understood that $\delta = 0$ is the case of a perfect periodic structure. For clarity of discussion, we introduce dimensionless frequency $\Omega_{L1} = \omega\overline{a}_1 / c_{L1}$ where c_{L1} is the longitudinal wave speed in the solid material.

The influences of the disordered degree on the band structures of the 1D ordered (the black solid line) and disordered (the blue dashed line and the red dotted line) PNCs for the wave incidence at an angle of 30° are described in Fig. 2. It can be seen from the figure that for 1D ordered solid-liquid PNCs the pass bands are narrower than the band gaps. For instance, consider the frequency intervals (0.725, 0.824) and (1.451, 1.495) (the zones marked by circles). It is observed that the location factor becomes positive in the pass bands (excluding the lowest pass bands) when δ is nonzero and increases in its value as δ increases. This behavior is the so-called localization of elastic waves. It should be noticed that there are two peaks at the frequencies 1.660 and 3.167 which means that the localization are stronger at these frequencies.

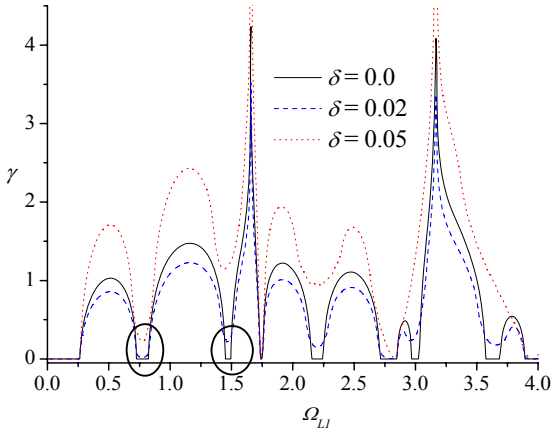

Figure 2 The influences of the disordered degree for the incident at an angle of 30°

Conclusions

The concept of the localization factor is introduced to describe the band structures and localization behaviors of 1D perfect and randomly disordered phononic crystals. The results show that the localization factor is an accepted and effective parameter in characterizing localization behavior of disordered phononic crystals. As the disorder of the system increase, the value of the localization factor increases in the bands. This localization behavior is more pronounced at higher frequencies.

Acknowledgements

The authors are grateful to the support by the National Science Foundation under Grant No.10902012 and 10632020.

References

[1] M. S. Kushwaha, P. Halevi, G. Martinez, L. Dobrzynski and B. Djafarirouhani, *Phys. Rev. Lett.* 71: 2022-2025(1993).
[2] A. Khelif, Y. Achaoui, S. Benchabane, V. Laude and B. Aoubiza, *Phys. Rev. B*, 81: 214303(2010).
[3] K. Huang and R. Q. Han, *Solid Physics*, Higher Education Press, Beijing (1988).
[4] P. W. Anderson, *Phys. Rev.* 109: 1492-1505(1958).
[5] E. L. Tan, *Ultrasonics*, 50: 91-98(2010).
[6] A. Wolf, J. B. Swift, H. L. Swinney and J. A. Vastano, *Phys. D*, 16: 285-317(1985).

Phononics 2011: First International Conference on Phononic Crystals, Metamaterials and Optomechanics
Santa Fe, New Mexico, USA, May 29-June 2, 2011
PHONONICS-2011-0084

Dynamic Imaging of Gigahertz Phonons on Phononic Crystal Slabs

Oliver B. Wright[1], Ryota Chinbe[1], Paul H. Otsuka[1], Motonobu Tomoda[1], Osamu Matsuda[1], Yukihiro Tanaka[1], Istvan A. Veres[2], Sihan Kim[3], Heonsu Jeon[3]

[1] Division of Applied Physics, Graduate School of Engineering, Hokkaido University, Sapporo 060-8628 Japan, assp@kino-ap.eng.hokudai.ac.jp
[2]Recendt, Research Center for Non Destructive Testing, Linz 4020, Austria
[3] Department of Physics and Astronomy and Inter-university Semiconductor Research Center, Seoul National University, Seoul 151-747, South Korea

Abstract: Surface phonon propagation on microscopic phononic crystal slabs of Si is dynamically imaged in two dimensions at frequencies up to 1 GHz by an ultrafast optical technique. The acoustic dispersion relations obtained by spatial and temporal Fourier transforms reveal stop bands and the eigenmode patterns. Phonon guiding and confinement in phononic crystal waveguides and cavities are also presented.

Surface acoustic wave devices based on one-dimensional (1D) periodic structures have found extensive application in high-frequency signal processing. 2D phononic crystals exhibit interesting physical properties, such as omnidirectional stop bands, that allow potential improvements to these devices. Here we present results of real-time imaging of optically-induced surface phonons at frequencies up to ~1 GHz in phononic crystal slab structures based on honeycomb lattices[1]. These structures exhibit complete stop bands for Lamb wave propagation.

We use optical pulses of duration ~200 fs, wavelength 830 nm and repetition rate 80 MHz from a Ti:sapphire femtosecond laser. A 415 nm pump beam derived from this laser excites phonon wave packets at a point on the sample surface by thermoelastic expansion. The 830 nm beam, after being delayed relative to the pump beam, is used to probe the sample with an interferometer. The beams are focused to spots of about 1 μm in diameter. The probe spot is scanned across the sample relative to the pump to generate images at various delay times over an area ~ 200×200 μm^2, allowing movies of the out-of-plane velocity of the surface motion to be obtained at acoustic frequencies up to ~ 1 GHz[2,3].

The samples are based on microscopic honeycomb lattices of circular holes patterned in (111) silicon-on-insulator wafers by a dry etching process. The silicon oxide (insulator) is then removed by wet

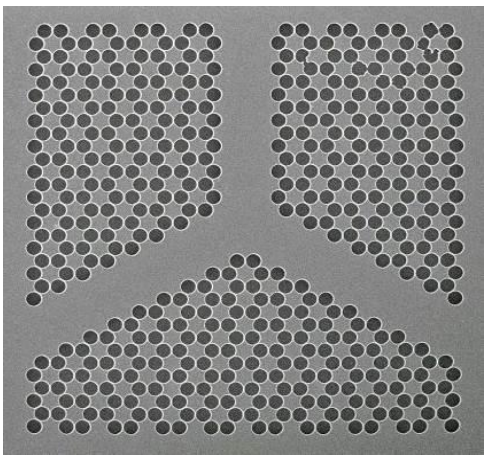

Figure 1 Electron microscope image of a (111) Si slab sample consisting of a Y-shaped waveguide formed by holes of diameter 5.8 μm arranged in a honeycomb lattice with center-to-center spacing 6.6 μm. The thickness of the slab is 6.5 μm.

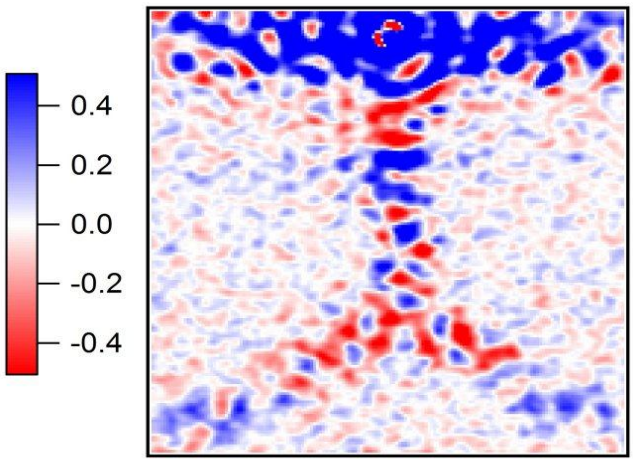

Figure 2 Corresponding image of the surface motion in the Y-shaped waveguide. The frequency is 322 MHz, lying at the top of the first stop band. A 200 × 200 μm^2 region is shown.

Phononics 2011: First International Conference on Phononic Crystals, Metamaterials and Optomechanics

Santa Fe, New Mexico, USA, May 29-June 2, 2011

PHONONICS-2011-0084

etching to leave free standing crystalline Si slabs of thickness 6.5 μm. A typical sample pattern, with the *x* axis corresponding in the [-2, 1, 1] direction of the crystal, is shown in Fig. 1; a Y-shaped region with no holes forms a phononic crystal waveguide. The center-to-center spacing of the holes is a=6.6 μm, whereas the diameter is $2r$=5.8 μm. The ratio r/a=0.44. The expected first complete phononic stop band lies between ~ 230 and 320 MHz for this phononic slab, as verified by simulations based on the orthogonal plane wave method.

Figure 2 shows a snapshot of a 200 μm square region of this sample at a frequency of 322 MHz. The excitation point is just outside the top end of the waveguide. This image was obtained from the temporal Fourier transform of time-domain data. Because this frequency corresponds to the top of the first stop band, the phononic waveguide transmits relatively efficiently.

We have in this way visualized the propagation of surface phonons in microscopic two-dimensional phononic crystals, phononic crystal waveguides and phononic crystal cavities based on this slab geometry. The dispersion relations, including stop bands, and the eigenmode patterns in two dimensions at individual frequencies are extracted by spatial and temporal Fourier transforms.

In addition we have conducted finite element time domain numerical simulations of phonon propagation in these phononic crystal structures that agree substantially with the experimental results. This work should lead to new diagnostic techniques for the propagation of surface acoustic waves in phononic structures, including surface acoustic wave devices[4].

References

[1] S. Mohammadi, A. A. Eftekhar, W. D. Hunt, and A. Adibi, *Appl. Phys. Lett* **94**, 051906 (2009).
[2] D. Profunser, E. Muramoto, O. Matsuda, O. B. Wright and U. Lang, *Phys. Rev. B* **80**, 014301 (2009).
[3] D. Profunser, O. B. Wright and O. Matsuda, *Phys. Rev. Lett.* **97**, 055502 (2006).
[4] T. Fujikura, O. Matsuda, D. M. Profunser, O. B. Wright, J. Masson, and S. Ballandras, *Appl. Phys. Lett.* **93**, 261101 (2008).

Phononics 2011: First International Conference on Phononic Crystals, Metamaterials and Optomechanics

Santa Fe, New Mexico, USA, May 29-June 2, 2011

PHONONICS-2011-0085

Observation and Simulation of Surface Acoustic Waves in Phononic Crystal

Paul H. Otsuka[1], István A. Veres[2], Keisuke Nanri[1], Sorasak Danworaphong[3], Motonobu Tomoda[1], Oliver B. Wright[1], Osamu Matsuda[1], Dieter Profunser[1], Abdelkrim Khelif[4], Vincent Laude[4], Sarah Benchabane[4]

[1]Graduate School of Engineering, Hokkaido University, Japan
paul@eng.hokudai.ac.jp
[2]Recendt, Research Center for Non Destructive Testing, Linz 4020, Austria
[3]School of Science, Walailak University, Thailand
[4]FEMTO-ST, Besancon, France

Abstract: We present an analysis of surface acoustic waves propagating in a microscopic phononic crystal waveguide consisting of a silicon crystal containing a square array of holes. Experiments are performed using an ultrafast optical method and the results are compared with an FEM simulation.

By modifying the structure inside a phononic crystal, waveguide devices that control the path of propagation of surface acoustic waves can be created[1,2]. Such devices are useful in signal processing and filtering applications. Optical generation and detection of surface waves has proved effective in visualising their propagation in real time[3,4]. We present results of real-time imaging and simulation of laser-induced surface acoustic waves at frequencies up to ~1 GHz in phononic crystals with a waveguide structure.

We generate and detect surface acoustic waves in phononic crystal waveguides using an optical pump-and-probe method[3,4]. The phononic crystals, made by deep reactive ion etching, contain microscopic circular holes 100 μm deep in (100) silicon arranged in a square array, with the waveguide channel formed by the absence of selected holes. The optical pulses used for excitation and detection are generated by a mode-locked Ti:sapphire laser. A 415 nm pump beam derived from this laser thermo-elastically excites the acoustic waves and an 830 nm probe beam delayed relative to the pump beam is used for detection with an interferometer. The optical pulse duration is ~200 fs and the repeti-

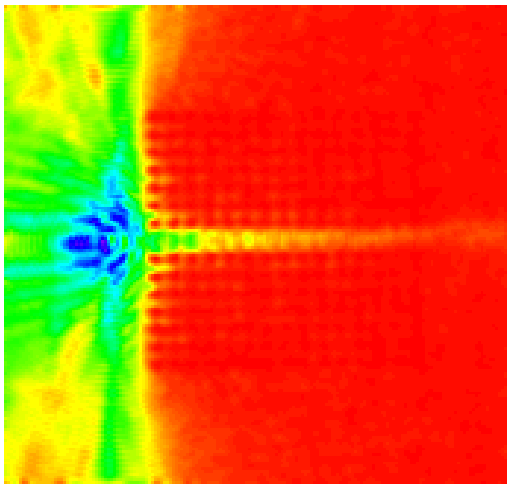

Figure 1 Experimental image of surface acoustic waves at 656 MHz propagating in a linear phononic crystal waveguide. Image size is 160×160 μm^2. The horizontal direction corresponds to the [011] crystalline direction.

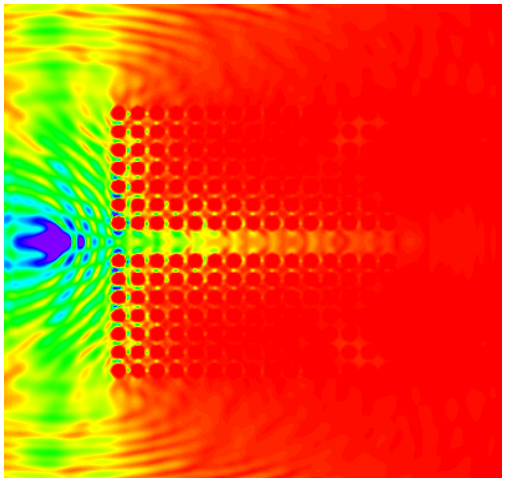

Figure 2 Simulation image of surface acoustic waves at 656 MHz propagating in a linear phononic crystal waveguide. Image size is 160×160 μm^2. The horizontal direction corresponds to the [011] crystalline direction.

Phononics 2011: First International Conference on Phononic Crystals, Metamaterials and Optomechanics
Santa Fe, New Mexico, USA, May 29-June 2, 2011
PHONONICS-2011-0085

tion rate is 80 MHz. The beams are focused to a spot of about 1 μm in diameter. The probe beam is scanned across the sample to generate images of regions of about 160×160 μm^2 in area. By varying the probe delay time, we build up animations of the surface waves propagating through the waveguides.

The experimental results are compared with a numerical simulation based on the Finite Element Method (FEM). The three-dimensional (3D) model consists of approximately 150 million nodes, and the resulting out-of-plane surface displacements are taken as the numerical counterpart of the experimental images. Movies of the surface wave propagation in the time domain are first obtained.

For both experiment and simulation results, we then use a dual Fourier transform method consisting of 1D temporal and 2D spatial Fourier transforms to extract the acoustic fields and slowness surfaces in 2D at individual frequencies. Time-resolved images reveal effects such as diffraction, refraction, reflection, resonance and waveguiding. The results show significant dependence of the wave propagation on frequency. In particular, the transmission through the waveguide channel shows peaks at particular frequencies. At other frequencies, there is strong attenuation due to the waves leaking into the phononic crystal region. Figure 1 shows the modulus of the experimentally measured field amplitude in a linear phononic crystal waveguide sample at 656 MHz. This frequency lies well above the first phononic stop band. The phononic crystal in this case is made up of a square lattice of circular holes with radius 6.5 μm, corresponding to a filling fraction of 70%. The pump pulses are focused at about 20 μm to the left of the opening of the waveguide, and the excited surface acoustic waves (SAW) propagate outwards from this point. Figure 2 shows the corresponding simulation results at the same frequency, exhibiting good agreement with the experiment. In both cases, there is significant attenuation of the excited waves in the waveguide channel. At other frequencies, for example at 328 MHz corresponding to the first phononic stop band, we observe much less attenuation in the waveguide.

This research allows the identification of the mechanisms responsible for the interaction of surface waves with phononic crystal devices, as well as being useful for the design and analysis of novel SAW waveguide devices.

References

[1] A. Khelif, A. Choujaa, S. Benchabane, B. Djafari-Rouhani, V. Laude, *Appl. Phys. Lett.* **84**, 4400 (2004).
[2] R. H. Olsson III, I. El-Kady, and J. G Fleming, *Sensors Actuators A*, **145–146**, 87 (2008).
[3] D. Profunser, E. Muramoto, O. Matsuda, O. B. Wright and U. Lang, *Phys. Rev. B* **80**, 014301 (2009).
[4] D. Profunser, O. B. Wright and O. Matsuda, *Phys. Rev. Lett.* **97**, 055502 (2006).

Phononics 2011: First International Conference on Phononic Crystals, Metamaterials and Optomechanics
Santa Fe, New Mexico, USA, May 29-June 2, 2011
PHONONICS-2011-0087

Evanescent Bloch Waves in Phononic Crystals: Complex Band Structure, Losses, and Guidance

Vincent Laude[1], Rayisa P. Moiseyenko[1,2]. Younes Achaoui[1], Sarah Benchabane[1], and Abdelkrim Khelif[1,2]

[1] *Institut FEMTO-ST, Université de Franche-Comté and CNRS, Besançon, France,*
vincent.laude@femto-st.fr, rayisa.moiseyenko@femto-st.fr, younes.achaoui@femto-st.fr, sarah.benchabane@femto-st.fr
[2] *Georgia Institute of Technology, GT-CNRS UMI 2958, Georgia Tech Lorraine, Metz, France*
akhelif3@mail.gatech.edu

Abstract: The complex band structure of evanescent Bloch waves in phononic crystals is elucidated by formulating an eigenvalue problem for the wavevector versus the frequency. It is used to explore the effects of material losses and the phononic crystal guidance mechanism. The method, originally formulated for plane waves, is extended to finite element models.

Phononic crystals are two- or three-dimensional periodic structures that consist of two materials with different elastic constants. They possibly give rise to absolute stop bands for a right choice of geometrical conditions and combination of materials. In addition, their unique dispersion properties can be used to design efficient waveguides, cavities or to obtain unusual refraction properties. Band structures are usually employed to describe infinite phononic crystals, as they provide information regarding any wave propagating in the periodic medium (Bloch waves). However, it is well-known that evanescent waves must be considered in propagation problems whenever scattering, diffusion, or diffraction by an object of finite size are investigated. In the context of phononic crystals, evanescent waves appear very naturally within frequency band gaps: since no waves can propagate within a band gap, only evanescent waves are left to explain the exponentially-decreasing transmission of acoustic waves. Furthermore, the mechanisms behind the creation of phononic crystal cavities and waveguides based on defects involve that only evanescent waves are present outside the defect, so that energy confinement can be guaranteed. A description of the effect of material losses on the propagation of elastic or acoustic waves can also be obtained – at least for incident monochromatic waves – by considering complex wavevectors.

In a recent paper[1], we extended the classical plane wave expansion (PWE) method so that it includes complex wave vectors in the direction of propagation. To do so, it is necessary to consider a fixed frequency and to solve for the wave vector $k(\omega)$, in contrast to the traditional way of obtaining band structures by considering any Bloch wave vector within the first Brillouin zone and solving for the frequency of allowed modes $\omega(k)$. The extended PWE method was used to generate band structures for two-dimensional solid-solid or solid-void phononic crystals. With the method, both propagative and evanescent solutions are found at once. The decay constants within band gaps are thus found and shown to depend on the wave polarization. Complex band structures also allow us to identify clearly the different branch systems in the band structure as these become continuous functions of the frequency. They also connect propagating bands below and above band gaps through evanescent bands, so that band folding can be unambiguously followed. Furthermore, the distribution of the acoustic fields of evanescent modes can be computed. Their transformation from below to above a band gap and within was shown to be perfectly continuous along the corresponding complex branch of the band structure.

As suggested above, complex band structures can be obtained for lossy phononic crystals. We have specifically considered the case of viscoelastic media. In order to include material damping, the rank-4 viscosity tensor η_{ijkl} is introduced. This tensor has the same symmetry as the elastic tensor c_{ijkl}. Attenuation can be assumed to increase linearly with frequency, as it proper to polymers but also to crystalline solids such as silicon, quartz or lithium niobate. For monochromatic waves, a complex-valued elastic tensor can then be written as $c_{ijkl} + i\omega\eta_{ijkl}$. More generally, any frequency dependent complex elastic tensor could be considered to model loss, without any further modification of the method. We have computed complex band structures via the extended PWE method for various phononic crystals, e.g. composed of steel rods in lossy epoxy[2] or of hollow holes in a silicon matrix, as depicted in Figure 1. Significantly, we have found that in contrast to homogeneous materials, the real part of the wavevector is more affected by losses than its imaginary part is. This effect is especially pronounced whenever the group velocity is small, for instance at the edges of a band gap. It also causes flat bands to acquire en-

Phononics 2011: First International Conference on Phononic Crystals, Metamaterials and Optomechanics

Santa Fe, New Mexico, USA, May 29-June 2, 2011

PHONONICS-2011-0087

hanced losses. Furthermore, the group velocity is limited by losses to finite values larger than zero, the value of the limit increasing with the level of viscosity.

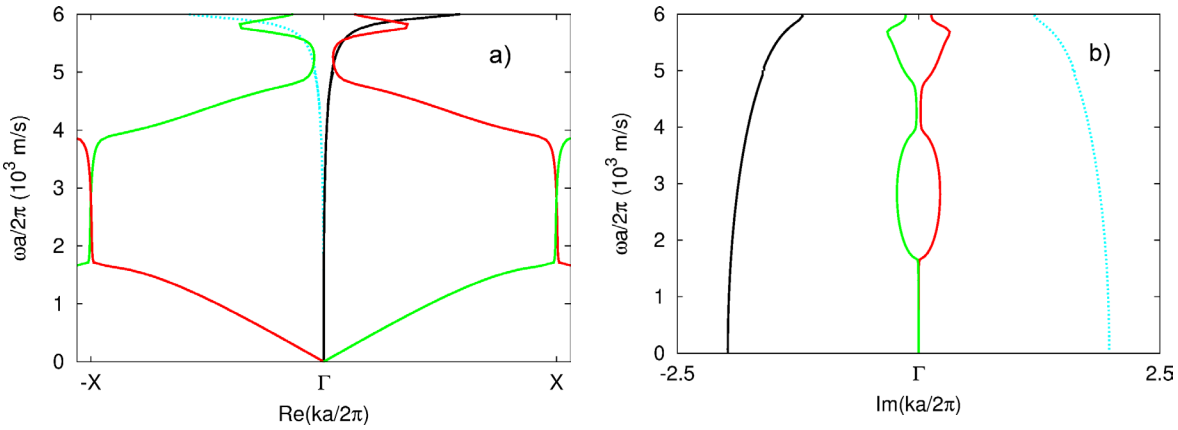

Figure 1 Complex dispersion relation computed with the EPWE method for a lossy square-lattice phononic crystal of silicon with cylindrical holes, with filling fraction 57%, and η44 = 0.08 Pa.s. In the complex band structure, the reduced frequency is presented as a function of (a) the real part and (b) the imaginary part of the wave vector. Only pure shear waves are shown for simplicity.

It is well known that the PWE method, though it is able to represent an almost arbitrary distribution of material constants within the unit-cell, can suffer in certain cases from some convergence problems or computational inefficiency. The finite element method (FEM) is also well suited to the representation of arbitrary material distributions, but is in contrast immune from the above detrimental effects. FEM is generally used to compute classical $k(\omega)$ band structures, but there is a strong interest to extend it to complex band structures. We introduce a general variational framework to obtain extended FEM algorithms. For definiteness, the popular example of two-dimensional phononic crystals of steel rods in water is considered. Complex band structures limited to purely longitudinal waves are obtained in this case.

After analyzing the perfectly periodic phononic crystal, we turn to the defect-based guidance mechanism. As argued above, guidance relies on the fact that all Bloch waves are evanescent in the phononic crystal surrounding the defect, providing the frequency falls within a complete band gap. A usual procedure is the super-cell technique, whereby a pseudo-periodic unit-cell is created by surrounding the defect with a few rows of phononic crystal. Computing the complex band structure for the super-cell gives a very precise understanding of the strength of the guidance (*via* the absolute value of the imaginary part of the wavevector for evanescent Bloch waves). Furthermore, the dispersion and the interaction of the different guided modes can be identified. We especially observe band gaps for guided modes that appear along the direction of the defect for frequencies within the two-dimensional phononic crystal complete band gap.

Financial support by the Agence Nationale de la Recherche under grant ANR-09-BLAN-0167-01 is gratefully acknowledged.

References

[1] V. Laude, Y. Achaoui, S. Benchabane, and A. Khelif, Phys. Rev. B **80**, 092301 (2009).
[2] R. P. Moiseyenko and V. Laude, to be published in Phys. Rev. B.

Phononics 2011: First International Conference on Phononic Crystals, Metamaterials and Optomechanics
Santa Fe, New Mexico, USA, May 29-June 2, 2011
PHONONICS-2011-0106

Demonstration of Ultra High Frequency Fractal Air/Aluminum Phononic Crystals

Nai-Kuei Kuo, Gianluca Piazza

University of Pennsylvania, Philadelphia, Pennsylvania 19103 , USA,
kuo1@seas.upenn.edu, piazza@seas.upenn.edu

Abstract: This work presents, for the first time, the design and the experimental demonstration of an air/aluminum nitride (AlN) phononic band gap (PBG) structure patterned in a fractal fashion which exhibits two frequency stop bands for symmetric lamb waves respectively at 900 MHz (bandwidth of 11%) and 1.075 GHz (bandwidth of 13.5%) with a maximum acoustic attenuation of 45 dB.

Thanks to the advancements introduced by microfabrication techniques, the research activities in phononic band gap (PBG) structures have recently matured from a theoretical exercise or the fabrication of hand-assembled components to the physical demonstration of large scale manufacturable structures operating in the high frequency range [1,2,3]. More intriguingly, recent experimental demonstrations have evolved to the point that realizing PBG-based devices, such as resonators [4,5] and waveguides [2], operating in the very high frequency (VHF) range is possible. However, in order to employ the PBG structures for commercial applications (*i.e.* wireless communications), it is necessary to expand the operation of these structures to a higher frequency range, which requires the miniaturization of the PBG unit cell. In this work, a novel fractal PBG structure design is introduced in order to operate in the ultra high frequency (UHF) range using a lithographically-defined minimum feature size of 0.7 μm. The unit cell consists of a center square with four smaller squares repeating at its four corners (Figure 1). Due to its unique geometry, the fractal PBG design prohibits the acoustic wave propagation of higher order modes of vibration (Figure 2) instead of the fundamental ones, which are generally blocked by the conventional circular scatterers distanced by the same pitch. Therefore, the fractal PBG enables operation at higher frequency for the same lithographically defined geometrical dimensions. To demonstrate a PBG structure in the range of 1 GHz, its key dimensions are designed to be: 5 μm for the lattice constant, *a*; 2 μm for the center square length, *c*; and 1.5 μm for the side square length (Figure 1), *s*. Lastly, the unit cell thickness is set to 1 μm in order to obtain sufficient electro-mechanical coupling for in-plane integration with the lamb wave transducers.

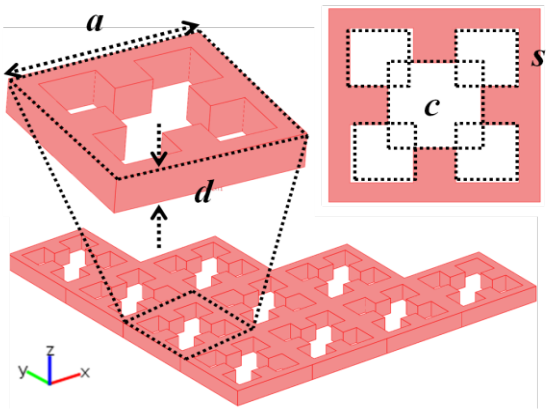

Figure 1 The array and unit cell of the fractal PBG structure with its physical key parameters: lattice constant, *a*, center square length, c, side square length, s, and thickness, *d*.

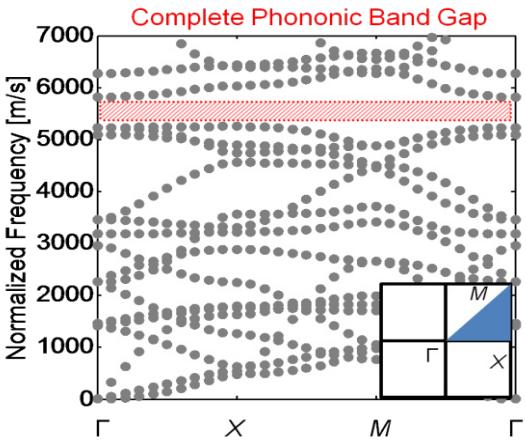

Figure 2 The dispersion relationship between the normalized frequency and the wave vectors in the reciprocal space of the first symmetric Brillouin zone. The red-shaded area is the complete frequency band gap displayed by the fractal structure with key parameter ratios $c/a = 0.44$, $s/c = 0.68$, and $d/a = 0.2$.

Experimental Results

In this experiment, AlN lamb wave transducers are integrated in the same plane of the PBG structure to efficiently launch longitudinal acoustic waves in the PBG (Figure 3a). 14 transducers were used to cover

Phononics 2011: First International Conference on Phononic Crystals, Metamaterials and Optomechanics
Santa Fe, New Mexico, USA, May 29-June 2, 2011
PHONONICS-2011-0106

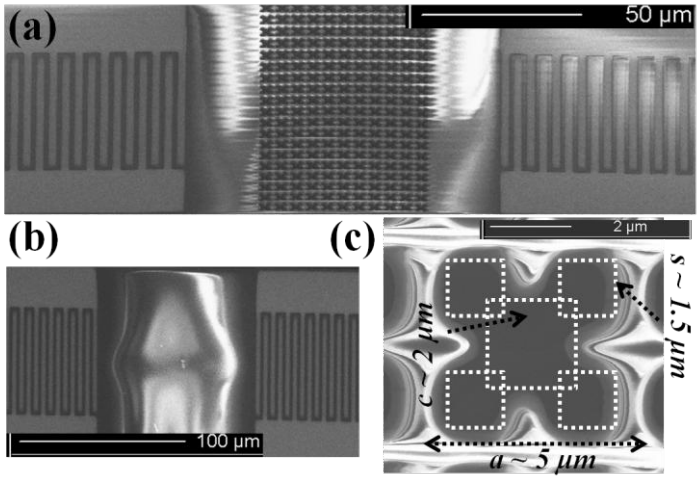

Figure 3 SEM images of : **(a)** the AlN lamb wave transducers and the fractal PBG array; **(b)** the AlN bulk acoustic delay-line used as reference device; **(c)** the zoomed-in view of the unit cell of the fractal PBG structure and its physical key parameters: a = 5 µm, c = 2 µm, s = 1.5 µm.

the frequency range of interest and extract the PBG response. The entire set of devices, the reference plate and the PBG were all simultaneously micro-fabricated in a post-CMOS compatible process (Figure 3). The AlN delay-line transducers were designed to serve as the reference of the acoustic responses (Figure 3b). The PBG response was measured via an Agilent N5230 PNA-L network analyzer after a standard short-open-load-through (SOLT) calibration. Approximately 4-5% bandwidth of each transducer was taken and summed to cover the entire frequency range of interest. Then, the PBG response was normalized with respect to the delay-line reference response. Figure 4 shows the existence of two frequency stop bands centered at 900 MHz and 1.075 GHz with bandwidths of 11% and 13.5%, respectively. The designed PBG structure exhibits a maximum acoustic attenuation of 45 dB. The experimental data were confirmed by means of COMSOL finite element methods (FEM). The eigenfrequency analysis in the FEM approach offers an efficient way to estimate the frequency of operation of the band gaps and the associated bandwidths.

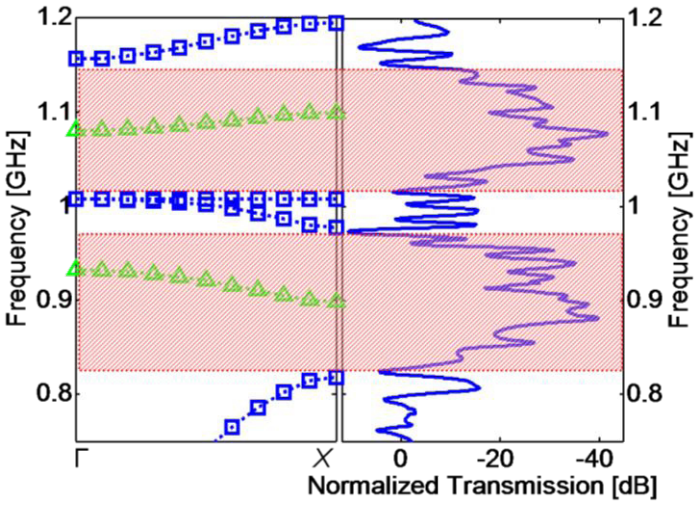

Figure 4 The COMSOL FEM dispersion curve versus the experimental normalized acoustic transmission of the PBG structure. Note: the blue square dotted lines represent the longitudinal modes; the green triangular dotted lines represent non-longitudinal ones (shear and transverse modes).

Conclusion

The operation of the fractal PBG design in air/aluminum nitride at 1 GHz has been experimentally demonstrated and confirmed by COMSOL FEM. Having reached the GHz range, it now becomes feasible to start considering the demonstrations of PBG-based RF devices for practical applications. Simultaneously, exotic PBG designs will be explored to further simply manufacturing processes in the UHF and SHF range.

References

[1] S. Mohammadi, et al., *Appl. Phys. Lett.*, **95**, 093501 (2008).
[2] R. H. Olsson III, et al., *Meas. Sci. Technol.*, **20**, 012002 (2008).
[3] N. Kuo, et al., *Appl. Phys. Lett.*, **95**, 093501 (2009).
[4] S. Mohammadi, et al., *Appl. Phys. Lett.*, **94**, 051906 (2009).
[5] C.-Y. Huang, et al., *Appl. Phys. Lett.*, **97**, 031913 (2009).

Phononics 2011: First International Conference on Phononic Crystals, Metamaterials and Optomechanics
Santa Fe, New Mexico, USA, May 29-June 2, 2011
PHONONICS-2011-0109

Ultrasonic Wave Transport in Phononic Crystals

J.H. Page[1], E.J.S. Lee[1], A. Sukovich[1], Hefei Hu[1], C. Qiu[2], Zhengyou Liu[2], Y. Tanaka[3], T. Okada[3], S. Tamura[3], B. Merheb[4], J-F. Robillard[5], J.O. Vaseur[5] and P.A. Deymier[4]

[1] Department of Physics and Astronomy, University of Manitoba, Winnipeg, MB Canada R2T 2N2
[2] Department of Physics, Wuhan University, Wuhan 430072, People's Republic of China
[3] Department of Applied Physics, Hokkaido University, Sapporo 060-8628, Japan
[4] Department of Materials Science and Engineering, University of Arizona, Tuscon AZ 85721 USA
[5] Institut d'Electronique, de Micro-électronique et de Nanotechnologie, UMR CNRS 8520, Cité Scientifique, 59652 Villeneuve d'Ascq Cedex, France
jhpage@cc.umanitoba.ca

Abstract: Ultrasonic experiments on phononic crystals provide a powerful method for investigating the profound effects of periodic structure on wave propagation. We summarize recent progress that has been achieved by combining experiments with multiple scattering theory and FDTD calculations to study bandgap, negative refraction and focusing phenomena.

Phononic crystals - periodic composite materials with lattice spacings comparable to the wavelength of acoustic or elastic waves – may be considered ideal systems for studying wave phenomena in periodic media. Ultrasonic techniques are well suited for investigating the properties of these materials since the wave field can be measured directly; thus, a rather complete picture of wave propagation is accessible, allowing the transmission coefficient, the dispersion relations, unusual refraction and focusing effects, and the dynamics of the wave fields to be investigated. We study high quality three- and two-dimensional crystals (Fig. 1), which are most often constructed by embedding mm-size monodisperse spheres or rods in a liquid or solid matrix. Such structures produce band gaps, at frequencies around 1 MHz, where wave propagation is inhibited, with transmission through crystals of finite thickness proceeding by tunneling[1]. While band gaps are most commonly produced by Bragg scattering, they can also occur by a hybridization mechanism, involving the coupling of a strong scattering resonance with the propagating modes of the embedding medium. We investigate these two types of band gaps in 2D crystals made from nylon rods immersed in water, where the lattice constant *a* can be tuned by changing the separation between the scatterers. Since the bandgap frequencies for these two types of gap depend differently on *a*, their different physical origins can be identified experimentally. We observe both types of gap separately, and also the competition between the hybridization and Bragg mechanisms when they occur at similar frequencies in the same crystals. Further confirmation of the different character of the hybridization gaps in our crystals is revealed by comparison with random samples, where the hybridization gaps persist but the Bragg gaps are destroyed. These data for the crystals and random systems are interpreted using Multiple Scattering Theory[2] and a Spectral Function Approach[3], yielding additional insight into the observed behaviour. We show that, typically, the group velocity is negative in a hybridization gap, but positive and large in a Bragg gap, providing a signature for distinguishing between hybridization and Bragg gaps in pulse propagation experiments.

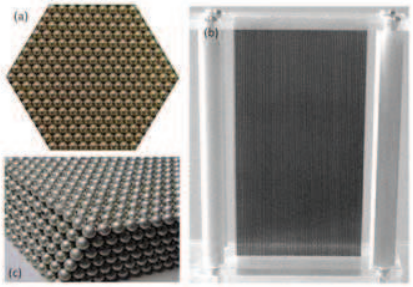

Figure 1 Some phononic crystals used in our ultrasonic experiments. (a) Top view of a fcc crystal of 1-mm-diameter tungsten carbide beads in water. (b) Front view of a triangular crystal of 1-mm-diameter steel rods, also immersed in water. (c) A mesoscopic opal made by brazing 4-mm-diameter aluminium beads in a fcc structure.

We also study mesoscopic opals – single-component phononic crystals made by brazing aluminum beads to form a solid face-centred-cubic structure that is more analogous to atomic crystals. In these crystals, the origin of the band gaps is different to the two cases considered above, being similar to the tight-binding model for electronic materials. The data are compared with predictions of Finite Difference Time Domain (FDTD) calculations, with good agreement being found for the frequencies at

Phononics 2011: First International Conference on Phononic Crystals, Metamaterials and Optomechanics
Santa Fe, New Mexico, USA, May 29-June 2, 2011
PHONONICS-2011-0109

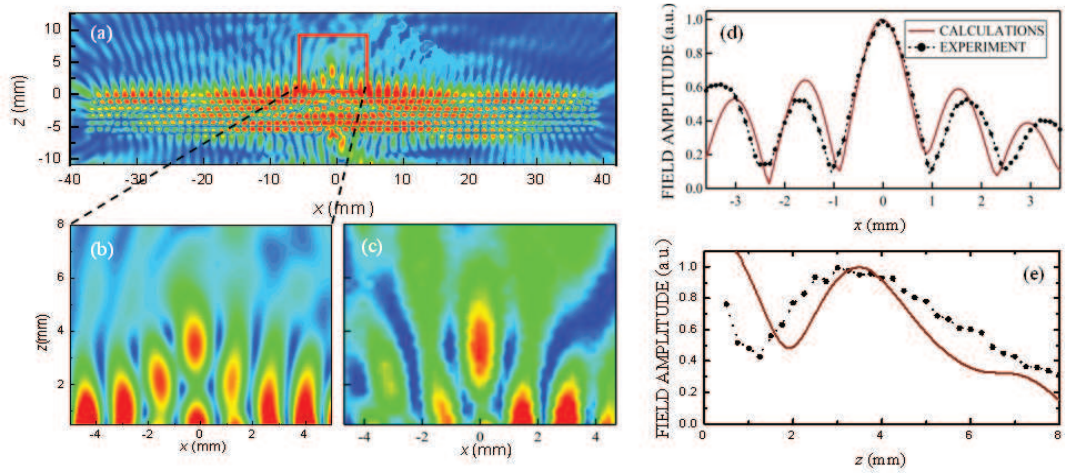

Figure 2 Super-resolution focusing of ultrasound at 530 kHz by a flat 2D phononic crystal consisting 1-mm-diameter steel rods arranged in a triangular lattice and immersed in methanol. The medium outside the crystal is water. (a) FDTD calculations of the average pressure amplitude when a 0.55 mm wide source is placed 0.1 mm below the surface of the crystal, at x = 0 mm and z = -6.35 mm. The crystal contains 6 layers of rods, with the output side of the crystal at z = 0. An image of the source is seen near x = 0 and z = 3.5 mm, as shown (b) and (c) for FTDT simulations and experiments, respectively. (d) and (e) Comparison of experiment and theory for the field amplitude through the peak of the focal spot along directions parallel and perpendicular to the lens surface. The experimental results and theoretical predictions for the half width of the focal spot parallel to the surface, $\Delta/2$, are found to be 0.37λ and 0.35λ.

which the band gaps occur. The bandgap properties of this crystal are contrasted with those of a disordered mesoglass, in which the most striking effect of disorder is three dimensional Anderson localization of ultrasound[4].

Since focusing of acoustic waves by negative refraction in flat phononic crystals was first demonstrated several years ago[5], there has been increasing interest in the possibility that focusing with resolution better than the diffraction limit of $\lambda/2$ may be achievable. In addition to demonstrating negative refraction directly, we show how super-resolution can be realized with two-dimensional phononic crystals in which the equifrequency contours are circular and well matched in size to the contours of the medium outside the crystal [6,7]. The phononic crystals are made of stainless steel rods assembled in a triangular crystal lattice and immersed in a liquid. To achieve matching of the equifrequency contours inside and outside the crystal, the liquid surrounding the rods in the crystal was chosen to be methanol, which has a lower sound velocity than the water outside. At a frequency close to that at which equifrequency contour matching occurs (0.55 MHz for this crystal), an image of a subwavelength source was obtained with a resolution of 0.37λ. Our experimental results are compared with theoretical predictions by the Finite Difference Time Domain (FDTD) method, which predicts an optimum resolution of 0.35λ – in good agreement to that observed experimentally (Fig. 2). Super-resolution imaging in these crystals is shown to be related to the coupling between the incident evanescent waves from the source and a bound slab mode of the phononic crystal lens, leading to amplification of evanescent waves by the slab mode. This phenomenon is only observed when the source is located very close to the lens and is very sensitive to the location of the source parallel to the lens surface, as well as to site disorder in the phononic crystal lattice. A simple model to predict the resolution limit is in good agreement with the experiments and FDTD simulations.

References

[1] Suxia Yang, J.H. Page, Zhengyou Liu, M.L. Cowan, C.T. Chan and Ping Sheng, *Phys. Rev. Lett.* **88**, 104301 (2002).
[2] J. Mei, Z. Liu, J. Shi, and D. Tian, *Phys. Rev. B* **67**, 245107 (2003).
[3] Xin Zhang, Zhengyou Liu, Fugen Wu, and Youyan Liu, *Physical Review E* **73**, 066604 (2006).
[4] H. Hu, A. Strybulevych, J.H. Page, S.E. Skipetrov and B.A. van Tiggelen, *Nature Physics* **4**, 945 (2008).
[5] Suxia Yang, J.H. Page, Zhengyou Liu, M.L. Cowan, C.T. Chan and Ping Sheng, *Phys. Rev. Lett.* **93**, 024301 (2004).
[6] A. Sukhovich, Li Jing and J.H. Page, *Phys. Rev. B* **77**, 014301 (2008).
[7] A. Sukhovich, B. Merheb, K. Muralidharan, J.O. Vasseur, Y. Pennec, P.A. Deymier and J.H. Page, *Phys. Rev. Lett.* **102**, 154301 (2009).

Phononics 2011: First International Conference on Phononic Crystals, Metamaterials and Optomechanics
Santa Fe, New Mexico, USA, May 29-June 2, 2011
PHONONICS-2011-0116

Locally resonant and Bragg band gaps for surface acoustic waves

Younes Achaoui[1], Abdelkrim Khelif [1,2], Sarah Benchabane[1], Laurent Robert[1], and Vincent Laude[1]

[1] *Institut FEMTO-ST, Université de Franche-Comté and CNRS, Besançon France*
younes.achaoui@femto-st.fr, sarah.benchabane@femto-st.fr, vincent.laude@femto-st.fr
[2] *International Joint Laboratory GeorgiaTech-CNRS UMI 2958; 2-3 Rue Marconi 57070 Metz, France*
akhelif3@mail.gatech.edu

Abstract: We investigate the propagation of surface acoustic waves in a square lattice phononic crystal of cylindrical pillars on an anisotropic substrate. It is shown that the propagation of surface acoustic phonons is prohibited in two distinct frequency ranges. We identify two mechanisms responsible for band gaps, i.e. local resonances and Bragg diffraction, and point out the difference between them.

The last years have seen a significant rise in the number of studies of band gap materials for acoustic waves. Basically, these artificial materials can be classified into two distinct families: phononic crystals[1] and acoustic metamaterials[2]. Indeed, they can both prohibit the propagation of acoustic waves in certain frequency ranges for all directions of incidence, but the physical phenomena behind are markedly different. The key parameter to obtain band gaps in the case of phononic crystals is periodicity, while the local frequency resonance of each basic cell dominates in the case of acoustic metamaterial. Furthermore, the position of band gaps in acoustic metamaterials can be significantly lower in frequency than the Bragg band gaps of phononic crystals. These sub-wavelength composites are good alternatives to overcome cumbersome devices in the sonic regime for instance.

Many works have been reported in the case of bulk waves for both phononic crystals and metamaterials. In the case of guided waves, drilling holes in a semi-infinite media as well as in thin plates was shown to prohibit the propagation of acoustic waves for wavelengths of the order of the lattice pitch[3,4]. More recently, low-frequency gaps and waveguiding in phononic crystals of pillars (or dots) on a plate have been demonstrated[5,6]. Here, we investigate experimentally the omnidirectional locally resonant and Bragg band gaps for surface acoustic waves on a semi-infinite substrate supporting a periodic array of pillars.

In our experiment, a square lattice array of cylindrical nickel pillars grown on a lithium niobate substrate has been considered. Surface acoustic waves are generated and detected using chirped interdigital transducers (CIDTs). These transducers are broadband sources placed on both sides of the periodic structure, as depicted in Figure 1. Several different samples have been fabricated in order to vary the direction of propagation and the investigated frequency range. Figure 2 shows examples of the ectrical transmission measured for propagation in the X-crystallographic direction using a network analyzer and radio-frequency probes. Figure 2-a and 2-b show the results obtained in two distinct frequency ranges. The red line shows the electrical response when no phononic crystal is present and is used as a reference. The green line shows the measurement in the presence of the phononic crystal.

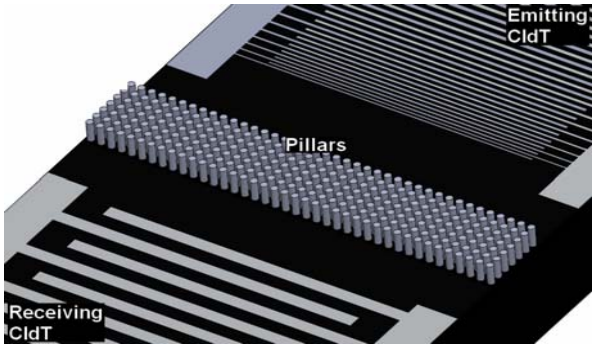

Figure 1 Schematics of the experimental setup used for investigating the interaction between the phononic crystal and surface acoustic waves. The periodic structure is a square lattice of nickel pillars grown on the surface of a lithium niobate substrate. Chirped interdigital transducers are placed on both sides for the emission and the detection of broadband surface acoustic waves using the piezoelectricity of lithium niobate.

Phononics 2011: First International Conference on Phononic Crystals, Metamaterials and Optomechanics
Santa Fe, New Mexico, USA, May 29-June 2, 2011
PHONONICS-2011-0116

With the periodic structure in between the two chirped transducers, we observe the appearance of a low frequency attenuation dip in the vicinity of 80 MHz (figure 2-a) and a second high frequency attenuation range in the vicinity of 140 MHz (figure 2-b). Transmission close to unity, i.e. with no noticeable loss, is observed between the two band gaps. Attenuation above 210 MHz is attributed to the conversion of guided modes to bulk waves propagating inside the substrate. The physical origin of the two gaps has been further investigated using optical interferometry. It is observed that the energy of surface waves is stored inside the pillars in the case of the low frequency gap, while the same waves are scattered on the surface in the case of the second band gap, leading to destructive interferences characteristic of the Bragg mechanism. We also obtained the group delay and the phase shift that is induced by the periodic structure on the propagation of surface waves.

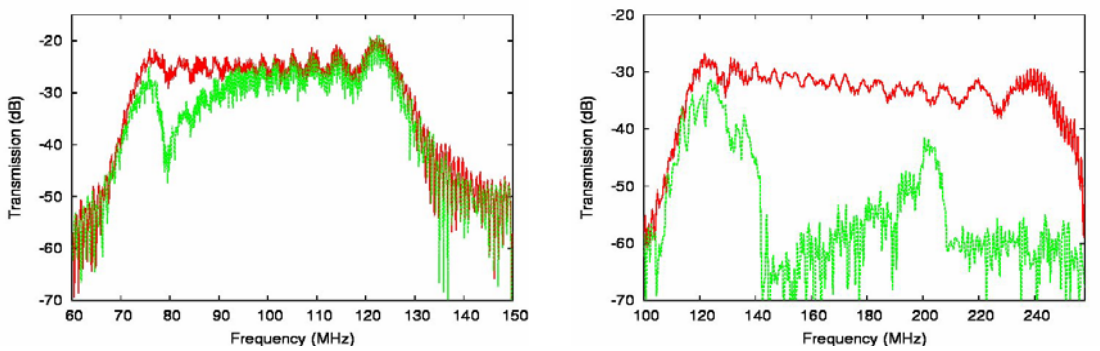

Figure 2 Measured electrical transmission using chirped interdigital transducers with (green line) and without (red line) the periodic structure in between. Case of (a) the locally resonant band gap (around 80 MHz) and (b) the Bragg band gap (around 140 MHz).

In order to account for the above results, we have computed dispersion curves and displacement field maps using a finite element method. We find that the pillars on the surface support locally resonant modes that extend inside the sound cone, and that band gaps for guided surface acoustic waves can be clearly defined.

According to our previous theoretical work[7], the main parameter that can shift in frequency the locally resonant band gap is the height of the pillars. Indeed, the locally resonant band gap is a consequence of the interaction of a resonance of the pillar with surface waves propagating on the substrate supporting the periodic structure. This resonance is also a function of the elastic constants of the pillars, of their mass density and of the geometrical details. For the same material choice, we have varied experimentally the height of the pillars and have monitored the corresponding change in the lower band gap frequency position. Increasing the height of the pillars results in a clear down-shift of the lower band gap, leading us to the conclusion that the latter results from a local resonance of the pillars.

Financial support by the Agence Nationale de la recherche under grant ANR-09-BLAN-0167-01 is gratefully acknowledged.

References :

[1] M.S. Kushwaha, P.Halevi, L. Dobrzynski, and B Djafari-Rouhani, Phys. Rev. Lett. **71**, 2022 (1993).
[2] Z. Liu, X. Zhang, Y. Mao,Y. Y. Zhu, Z. Yang, C. T. Chan, and P. Sheng, Science **289**, 1734 (2000).
[3] S. Benchabane, L. Robert, J.-Y. Rauch, A. Khelif, and V. Laude, Phys. Rev. E **73**, 065601 (R) (2006).
[4] S. Mohammadi, A. Eftekhar, W. Hunt, and A. Adibi, Appl. Phys. Lett. **94**, 104301 (2009).
[5] T.-T Wu, Z.-G Huang, T.C Tsai, and T.-C. Wu, Appl. Phys. Lett. **93**. 111902 (2008).
[6] Y. Pennec, B. Djafari-Rouhani, H. Larabi, J. O. Vasseur, and A. C. Hladky-Hennion, Phys. Rev. B **78**, 104105 (2008).
[7] A. Khelif, Y. Achaoui, S. Benchabane, V. Laude, and B. Aoubiza, Phys. Rev. B **81**, 214303 (2010).

Phononics 2011: First International Conference on Phononic Crystals, Metamaterials and Optomechanics
Santa Fe, New Mexico, USA, May 29-June 2, 2011
PHONONICS-2011-0127

Focusing and Waveguiding of Lamb Waves in Phononic Plates

Tsung-Tsong Wu, Jia-Hong Sun, Yan-Ting Chen
Institute of Applied Mechanics, National Taiwan University, Taipei, Taiwan
wutt@ntu.edu.tw

Abstract: In this talk, focusing of Lamb waves using the GRIN PC will be introduced first, and then followed by a concept demonstration of utilizing the focusing feature to compress Lamb waves into a phononic plate waveguide. Results of the study showed that beam width of the lowest anti-symmetric Lamb wave in a silicon PC thin plate can be compressed efficiently and fitted into the tungsten/silicon PC plate waveguide over a wide range of frequency.

Propagation of Lamb waves in thin plates with phononic crystal (PC) structures has attracted much interest due to the existence of absolute band gap (ABG) and the potential applications in filters, resonators, and waveguides in the past couple of years.[1-3] In comparison to the ABG, researches on the negative refraction and focusing of waves in phononic thin plates have just been started recently. Preliminary results showed that focusing of Lamb waves in thin plate can be achieved either by the negative refraction or using the gradient-index (GRIN) PC structure.[4,5]

In this talk, focusing of Lamb waves due to the features of GRIN PC will be introduced first, and then a concept demonstration of utilizing the focusing features to compress Lamb waves into a phononic plate waveguide. The band structure of an air/silicon PC plate (thickness:50 μm, lattice constant a =100μm and, radius r =40μm) with square lattice was studied and the equal frequency contours (EFCs) of the lowest anti-symmetric mode (A_0), the symmetric mode (S_0) and shear horizontal mode (SH_0) are shown in Figure 1. The results revealed that the A_0 mode is close to a circle (i.e., behave like an isotropic medium), while the S_0 and SH_0 modes are rather anisotropic. Figure 1 is the equal frequency contours (EFCs) evaluated at 3 MHz.

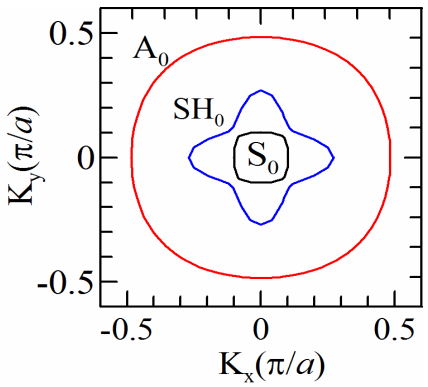

Figure 1 The equal frequency contours of the lowest anti-symmetric mode (A_0), symmetric mode (S_0) and shear horizontal mode (SH_0).

To design a GRIN PC plate for focusing the A_0 mode, we chose a refractive index profile in the form of a hyperbolic secant as[6]

$$n(y) = n_0 \operatorname{sech}(\alpha y) \tag{1}$$

where n_0 is the refractive index along the center axis (x-axis) and α is the gradient coefficient. For small anisotropic ratio and the overall waves propagating along the x-direciton, the refractive index of the A_0 mode was approximated by the refractive index along the ΓX direction as

$$n = \frac{v}{v_{\Gamma X}} = \frac{v}{d\omega / dk_{\Gamma X}}. \tag{2}$$

where $v_{\Gamma X}$ is the group velocity along the ΓX direction and v is the referenced group velocity of the A_0 mode of a homogeneous silicon plate with the same thickness (evaluated at 3 MHz). Consider a GRIN PC contained 15 rows of air holes (y= [−7 a, +7 a]) arranged in square lattice with graded filling fractions and operated at 3 MHz. By setting the radii of the holes at the center row (y = 0) and the boundary rows (y= ±7 a), the gradient coefficient can be determined accordingly.

Phononics 2011: First International Conference on Phononic Crystals, Metamaterials and Optomechanics
Santa Fe, New Mexico, USA, May 29-June 2, 2011
PHONONICS-2011-0127

To demonstrate the focusing of Lamb wave in the designed GRIN PC plate, numerical simulations were conducted with a line source placed at x= -2a. The result showed focusing of the wave beam along the propagation direction and reach maximum amplitude at x=28a approximately, and then, diverging out again. The simulation results also showed that the neck of the focus region extends for a long distance, which started from around 22a to 34a in this case.

To test the feasibility of compressing the wave beam of a plate wave into a wave guide with small aperture, the GRIN PC plate was terminated at x=22a and utilized as a beam width compressor. A phononic plate waveguide formed by removing one layer of cylinders from a silicon PC plate with periodic stubbed tungsten cylinders[7,8] (square lattice) on one of the plate surfaces was employed. By choosing the lattice constant of the PC waveguide as 150 μm and the radius and height of the tungsten cylinders as 36 μm and 273 μm, respectively, a complete band gap can be found in the range of 2.6-3.4 MHz. Figure 2 shows a combination of the GRIN PC beam width compressor and the aforementioned PC waveguide. The simulation result for operating frequency at 3 MHz demonstrates that the compressing and guiding of the wave beam into the designed waveguide can be achieved successfully. By taking the amplitude of the line source as unit, the result shows that the amplitude at the entrance of the waveguide is amplified to about 3.2. In addition, after propagating for a distance of 15 a in the waveguide, the wave amplitude still preserve a value of 2.8. Since the aperture of the line source is $15a$, the results showed that the FWHM of the compressing is about 17.3%. To demonstrate that the proposed GRIN PC plate focusing device is suitable for compressing wave with a range of frequency, numerical simulations with operating frequencies at 2.7 and 3.4 MHz were also conducted and the results showed that the focusing and compressing of Lamb waves are still valid with the amplitudes at the entrance of the waveguide equal to 2.5 and 2.6, respectively.

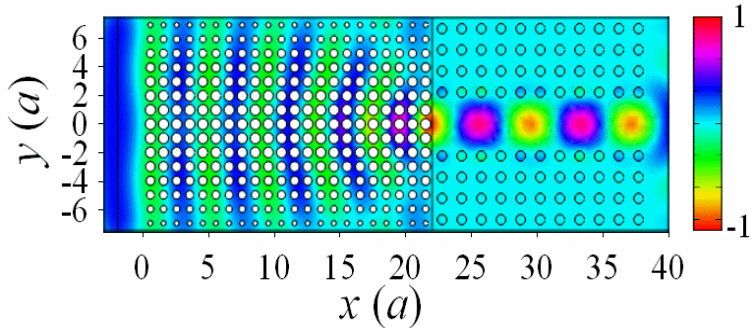

Figure 2 Simulation of the wave propagation along the x-direction in a GRIN PC plate adjoined with a PC plate waveguide at 3 MHz.

In summary, focusing of Lamb wave can be achieved by using a GRIN air/silicon PC thin plate. The refractive index profile in the form of a hyperbolic secant can be utilized approximately to design the GRIN PC plate. The results showed that the beam width of the lowest anti-symmetric Lamb mode can be compressed efficiently over a range of frequency and can potentially be utilized as a beam width compressor for compressing Lamb waves into a PC plate waveguide in the MEMS area.

References

[1] R. H. Olsson III, I. F. El-Kady, M. F. Su, M. R. Tuck, and J. G. Fleming, *Sensors and Actuators A* **145**, 87-93 (2008).
[2] S. Mohammadi, A. A. Eftekhar, W. D. Hunt, and A. Adibi, *Appl. Phys. Lett.* **94**, 051906 (2009).
[3] C.-Y. Huang, J.-H. Sun, and T.-T. Wu, *Appl. Phys. Lett.* **97**, 031913 (2010).
[4] M. Farhat, S. Guenneau, S. Enoch, A. B. Movchan, and G. G. Petursson, *Appl. Phys. Lett.* **96**, 081909 (2010).
[5] T.-T. Wu, Y. T. Chen, J. H. Sun, S.-C. S. Lin, T. J. Huang, submitted to *Appl. Phys. Lett.*
[6] S.-C. S. Lin, T. J. Huang, J.-H. Sun, and T.-T. Wu, *Phys. Rev. B* **79**, 094302 (2009).
[7] T.-C. Wu, T.-T. Wu, and J.-C. Hsu, Phys. Rev. B **79**, 104306 (2009).
[8] Y. Pennec, B. Djafari Rouhani, H. Larabi, A. Akjouj, J. N. Gillet, J. O. Vasseur, and G. Thabet, *Phys. Rev. B* **80**, 144302 (2009).

Phononics 2011: First International Conference on Phononic Crystals, Metamaterials and Optomechanics
Santa Fe, New Mexico, USA, May 29-June 2, 2011
PHONONICS-2011-0147

Multi-Objective Optimization of Phononic Bandgap Materials for Wide Band, Low Frequency Operation

Raymond A. Wildman and George A. Gazonas

Weapons and Materials Research Directorate, U.S. Army Research Laboratory,
Aberdeen Proving Ground, MD, USA
raymond.a.wildman@us.army.mil, george.aristotle.gazonas@us.army.mil

Abstract: Phononic bandgap materials are optimized for maximization of bandgap size and minimization of center frequency using a genetic programming method for inclusion shape design and material choice. Maximizing the bandgap size allows for a material design that can block a wide range of frequencies. Minimizing the center frequency will give designs that are small compared to the effective wavelength.

Phononic crystals have received much attention for their interesting properties, in fact, material choice and geometry can be engineered to obtain band stop filters[1], negative bulk properties[2], and cloaking[3]. Here, we wish to optimize two goals simultaneously: bandgap size and center frequency. Maximizing the bandgap size allows for structures that can block a wide range of frequencies. In many instances, a narrowband filter is of little use. The second goal is to minimize the center frequency of the bandgap. The center frequency determines the absolute range of frequencies that will be blocked. Seeking a low center frequency will yield a material that blocks propagating waves that have long wavelengths compared to the unit cell size, ultimately leading to smaller structures.

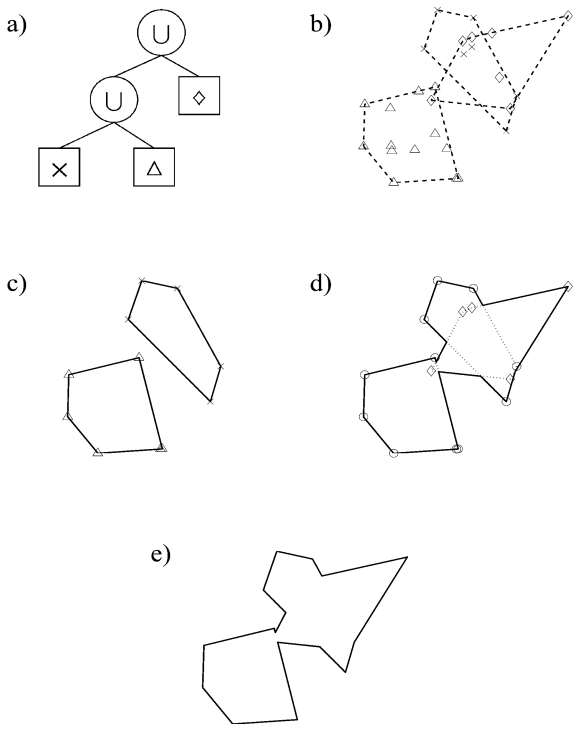

Figure 1 Decoding process. **(a)** Tree representation of a Boolean expression. **(b)** Point lists with their convex hulls, corresponding to leaf nodes in the tree. **(c)** Union of the left-most subtree. **(d)** Union of the result of **(c)** with remaining leaf node. **(e)** Final result.

Multi-objective optimization of phononic crystals has been discussed previously[4], where those authors optimized one dimensional structures for optimal pass-band and stop-band operation. Here, we optimize two dimensional, elastic structures using a genetic programming approach[5] and allow the optimizer to choose among several materials. The materials chosen are based on those that have been shown to lead to low frequency operation[6]. Results show that a set of Pareto optimal designs can be achieved for wide band and low frequency operation.

Optimization Method

Genetic programming (GP) is an optimization method derived from genetic algorithms (GAs), but uses a tree shaped chromosome to represent computer programs or general mathematical expressions. It has also been adapted to optimize geometry and topology in a general way[5]: As shown in Figure 1, Boolean expressions can be used to combine convex polygons, generating complex geometries from a few simple building blocks. In this approach, the convex polygon operands are represented as the convex hull of a list of points. A few advantages include: representation of large homogeneous regions with a small number of parameters, representation of both sharp corners and smooth regions, and

Phononics 2011: First International Conference on Phononic Crystals, Metamaterials and Optomechanics
Santa Fe, New Mexico, USA, May 29-June 2, 2011
PHONONICS-2011-0147

adaptability to inhomogeneous geometries.

Genetic algorithms (and by extension genetic programming) are well-suited to multi-objective problems because they already use a population of potential solutions. There have been many examples of multi-objective GAs, of which Ref. 4 is an example. Implementing Pareto optimization in a GA only involves changes to the selection operator, so any GP implementation is identical.

In contrast to Ref. 5, this application benefits from inhomogeneous structures[7]. Optimizing inhomogeneous structures using genetic programming requires a few modifications to the chromosome of Ref. 5. First, Boolean operations are no longer applicable because we require the operands to have some material properties. Instead, we apply an overlapping scheme based on a priority value (real valued and rounded to the nearest integer before use) stored in each operand. Given a sub-tree with two convex polygon operands, the operand with the higher priority is placed on top of the other. If two operands have identical priority values, then the union is used, taking the material properties from the left operand. The priority values, as well as the material values, are involved in crossover and mutation. In this application, a database of materials will be used rather than allowing the optimization scheme to vary the actual bulk material properties as in Ref. 7.

Forward Problem

The forward problem is based on formulating the elastic wave equation as an eigenvalue problem, so that a band diagram can be computed[1]. Essentially, Floquet boundary conditions are applied to two edges of a square unit cell and the elastic wave equation is discretized using linear finite elements. After testing and basis function substitution, a matrix equation is formed

$$\boldsymbol{Ax} = \omega \boldsymbol{Bx}, \tag{1}$$

which is a generalized eigenvalue problem in ω and $\boldsymbol{x}$. A local search algorithm is applied to find the lower band maximum ω_1 and upper band minimum ω_2, which gives the relative bandgap size

$$\frac{\omega_2 - \omega_1}{\sqrt{\omega_1 \omega_2}}, \tag{2}$$

and center frequency

$$\frac{\omega_1 + \omega_2}{2}. \tag{3}$$

Results

Pareto optimization was applied for the simultaneous optimization of bandgap size and center frequency using three materials: epoxy, lead, and silicone rubber[6]. The epoxy is fixed as the matrix material, and the algorithm is free to choose among it and the lead and rubber to form the inclusions.

Initial generations show two distinct clusters of (Pareto optimal) designs based on material: designs using lead show high center frequency and bandgaps, and designs using the rubber show the opposite. As the algorithm combines materials, the Pareto front (shown in Figure 2 as the "o" after 95 generations) begins to fill. Full results will be given at the conference.

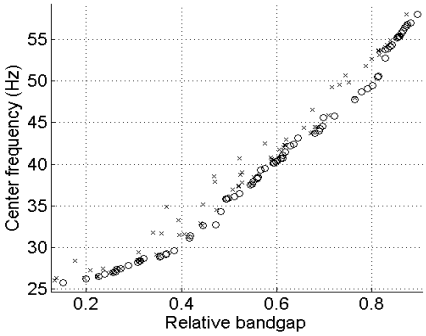

Figure 2 Pareto curve (o) after 95 generations

References

[1] G.A. Gazonas, D.S. Weile, R.A. Wildman, and A. Mohan, *Int. J. Solids Struct.* **43**, 5852-5866 (2006).
[2] J. Li and C.T. Chan, *Phys. Rev. E* **70**, 055602 (2004).
[3] Y. Cheng, F Yang, and J.Y. Xu, *Appl. Phys. Lett.*. **92**, 151913 (2008).
[4] M.I. Hussein, K. Hamza, G.M. Hulbert, R.A. Scott, and K. Saitou, *Struct. Multidisc. Optim.* **31**, 60-75 (2006).
[5] R.A. Wildman and D.S. Weile, *IEEE Trans. Antennas Propag*. **55**, 629-636 (2007).
[6] Z. Liu, X. Zhang, Y. Mao, Y.Y. Zhu, Z. Yang, C.T. Chan, and P. Sheng, *Science* **289**, 1734-1736 (2008).
[7] R.A. Wildman and D.S. Weile, *Electromagnetics* **30**, 222-236 (2010).

Phononics 2011: First International Conference on Phononic Crystals, Metamaterials and Optomechanics
Santa Fe, New Mexico, USA, May 29-June 2, 2011
PHONONICS-2011-0149

Resonance in *m*-layered Goupillaud-type Elastic Media

George A. Gazonas[1] and Ani P. Velo[2]

[1] *Weapons and Materials Research Directorate, U.S. Army Research Laboratory, Aberdeen Proving Ground, MD, USA, george.aristotle.gazonas@us.army.mil*
[2] *Department of Mathematics and Computer Science, University of San Diego, San Diego, CA 92110, USA, avelo@sandiego.edu*

Abstract: Explicit analytical and recursive stress solutions and corresponding natural frequencies are derived for an *m*-layered Goupillaud-type elastic medium from a coupled first-order system of difference equations using *z*-transform methods. The exact solutions can serve to verify computational methods for modeling wave propagation phenomena such as resonance and bandgap formation in periodic media.

The study of natural vibrations in elastic media include the study of resonance, as resonance can enhance the performance of many sensors and devices, yet can devastate structures subjected to sustained temporally-periodic loading. Despite the long history of developments in the field, exact solutions for the natural modes of vibration and the resonance response of multilayered (*m*-layered) elastic media have been primarily limited to the analysis involving only a few layers. Laplace transform methods are used in Ref. 1 to derive the transient resonance response of a free-fixed elastic bar; the analytical solution consists of a product of a temporal term and time-harmonic function in the solution, which becomes unbounded at large times. Ref. 2 provides closed-form, time-domain expressions for transient waves in an *m*-layered elastic medium, with an illustration of the transient resonance response of a single isotropic elastic layer sandwiched between two half-spaces that is subjected to a temporally periodic sawtooth function. Ref. 3 studies the natural frequencies of anisotropic *m*-layers, and illustrates beat phenomena in two and three layer systems using an efficient numerical eigensolution scheme that is based on semi-analytical methods. Exact expressions for the reflection coefficients for a two-dimensional elastic layer overlying an elastic half-space are obtained in Ref. 4, but the transient response of the system at resonance is not analyzed. A general method to determine the natural frequencies of composite rods for power ultrasonic applications with a specific solution for a two-rod system is presented in Ref. 5. The method can be extended to *m*-layered systems, but the general problem of determining the natural frequencies of arbitrary layer-thickness and material properties can only be solved using numerical methods. Exact analytical expressions are derivable, however, for the transient resonance response of an *m*-layered medium if we specialize the medium to be of Goupillaud-type[6]. Both recursive relations and explicit analytical expressions are derived that are exact for discretely layered and periodic media of Goupillaud-type (Figure 1); such solutions are invaluable for verification of computational methods involving transient of wave phenomena in such media. A related inverse problem in reflection seismology for finding the coefficients of a first order 2 *x* 2 hyperbolic system is treated in Ref. 7. In order to numerically solve the continuous initial-boundary-value problem, several difference schemes (stencils) are applied as discretizations to the corresponding differential equations. The difference scheme IVp, given in equation (3.1.11), pg. 517 of Ref. 7 is similar to our recursive relations (1) derived using the method-of-characteristics.

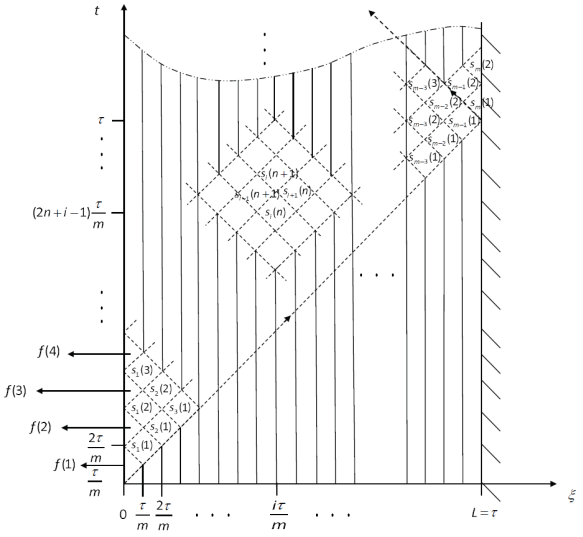

Figure 1 Lagrangian diagram for an elastic *m*-layered medium of equal wave travel time (Goupillaud-type medium) subjected to an arbitrary, discrete input *f(n)* on the left boundary and fixed on the right boundary.

Phononics 2011: First International Conference on Phononic Crystals, Metamaterials and Optomechanics
Santa Fe, New Mexico, USA, May 29-June 2, 2011
PHONONICS-2011-0149

Resonance in *m*-layers

Explicit analytical stress solutions are derived from a coupled first-order system of difference equations (1) using z-transform methods, and the determinant of the global system matrix $|A_m|$ in the z-space is a palindromic polynomial with real coefficients; the zeros are distinct and proven to lie on the unit circle for $1 \le m \le 5$ layers (Ref. 8), and for certain classes of m-layered designs of tridiagonal Toeplitz variety, i.e., continuants (Ref. 9). Stresses $s_i(n)$ in the layers with impedance contrast $\alpha_i = c_i\rho_i / c_{i+1}\rho_{i+1}$ due to loading $f(n), n \ge 1$ are given with reference to Figure 1 as,

$$
\begin{aligned}
s_1(n+1) &= -s_1(n) + \frac{2\alpha_1}{1+\alpha_1} s_2(n) + \frac{2}{1+\alpha_1} f(n+1), \\
s_2(n+1) &= -s_2(n) + \frac{2\alpha_2}{1+\alpha_2} s_3(n) + \frac{2}{1+\alpha_2} s_1(n+1), \\
&\cdots \\
s_{m-1}(n+1) &= -s_{m-1}(n) + \frac{2\alpha_{m-1}}{1+\alpha_{m-1}} s_m(n) + \frac{2}{1+\alpha_{m-1}} s_{m-2}(n+1), \\
s_m(n+1) &= -s_m(n) + 2s_{m-1}(n)\,.
\end{aligned}
\tag{1}
$$

Resonance frequencies $\omega_k = \arg z_k$, $1 \le k \le \left\lfloor \frac{m}{2} \right\rfloor$ are identified as the zeros of the determinant of m-layered tridiagonal Toeplitz systems found from z-transform of (1) above as,

$$
z_k = 2\varsigma\Theta - 1 \pm 2i\sqrt{\varsigma\Theta(1-\varsigma\Theta)}, \qquad \Theta = \cos^2\frac{\pi k}{m+1}\,, \qquad 0 < \varsigma < 1\ . \tag{2}
$$

A particular resonance response generated through sinusoidal loading of the boundary is shown in Figure 2; current efforts are focused on determining the limitations in using finite system (1) to generate acoustic bandgaps for infinite periodic media such as those investigated in Ref. 10, Figure 3.

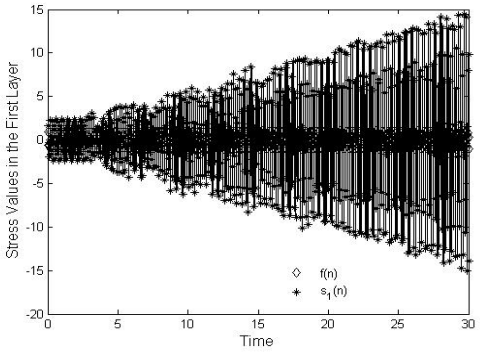

Figure 2 Resonance response of Layer 1 in a *47*-layered medium; stress values formed from interlacing sequences: $f(n) = \sin(n\omega_k)$, and $s_1(n)$, $k = 9, \varsigma = 1/2$.

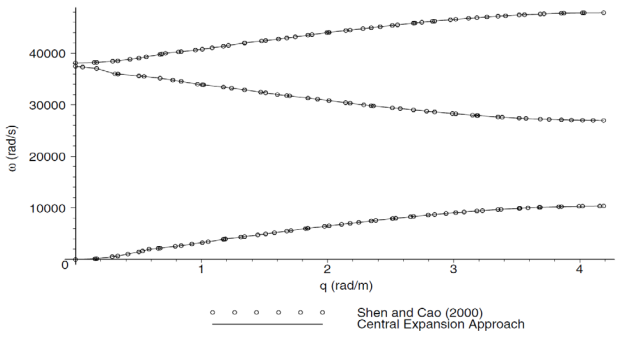

Figure 3 Dispersion graphs showing acoustic bandgap formation in a three-material unit cell (after Ref. 10).

References

[1] R.R. Churchill, *Operational Mathematics,* McGraw-Hill, NY (1972).
[2] G. Caviglia, and A. *J.* Morro, *Acous. Soc. Am.* **116(2)**, 643–654 (2004).
[3] J. Kaplunov, and A. Krynkin, *J. Sound Vibrat.* **294**, 663–677 (2006).
[4] M.S. Fokina, and V.N. Fokin, *J. Comput. Acoust.* **9(3)**, 1079–1093 (2001).
[5] K.F. Graff, *Wave Motion in Elastic Solids,* Dover Publications, NY (1975).
[6] P. Goupillaud, *Geophysics,* **36** 754–760 (1961).
[7] K. Bube, and R. Burridge, *Siam Rev.* **25(4)**, 497–559 (1983).
[8] G.A. Gazonas, and A.P. Velo, *(in review),* (2011).
[9] T. Muir, *A Treatise on the Theory of Determinants*, Dover Publications, NY (1960).
[10] A.P. Velo, G.A. Gazonas, E. Bruder, and N. Rodriguez, *Siam J. Appl. Math.* **69(3)**, 670–689 (2008).

Phononics 2011: First International Conference on Phononic Crystals, Metamaterials and Optomechanics
Santa Fe, New Mexico, USA, May 29-June 2, 2011
PHONONICS-2011-0152

On the Validity of 2D Numerical Simulation of Bandgap for Slab of Phononic Crystals

S. Alaie[1] , I. El-Kady[2], Z.C. Leseman[1]

[1] *Mechanical Engineering, University of New Mexico, Albuquerque, NM USA 87131*
alaie@unm.edu, zleseman@unm.edu
[2] *Sandia National Laboratories, , Albuquerque, NM US 87105*
ielkady@sandia.gov

Abstract: This work suggests a criterion for verification of Phononic bandpaps simulated by two dimensional elastodynamic models. The bandgap of a phononic crystals (PnCs) was studied using both 2D and 3D finite element analyses. Comparing the numerical results with experiment, this study indicates that validity of 2D models depends on the ratio of the thickness to the excitation wavelength.

In order to attain a fast estimation of bandgaps in PnCs, simulation of an infinitely thick model is an alternative to finite thickness models[1]. In order to reduce the three-dimensional equations to those for a two-dimensional model, plane stress condition is a common assumption employed in elastic media[2]. Since in the two dimensional analysis the degrees of freedom (DOFs) for each node is 2, and the model is limited to an area instead of a volume, this model is computationally cheaper than 3D models. In this model the medium is assumed so thin such that the out-of-plane components of stress vanishes[2]. However this assumption leads to neglecting out-of-plane modes in vibration of PnCs. In this paper a PnC, consisting a silicon dioxide and tungsten inclusions, is studied using 3D and 2D harmonic finite element analyses (HFEAs). Results of the current analyses are verified by comparing them to experimental results[3]. This study evaluates the efficiency and inefficiencies of these methods for prediction of phononic bandgap.

In harmonic analysis the governing equations are solved in the frequency domain and the steady state solution is attained without time discretization[4,5]. In order to apply the boundary conditions, a set of nodes are harmonically excited at a discretized range of frequencies. Consequently, the transmission spectrum of a PnC is achieved using the steady state solutions to the PnC model under line excitation in 2D model or surface excitation in 3D model (See Fig. 1). In Fig. 1 the current three dimensional numerical space is illustrated. The phononic crystal consists of one row of 19 tungsten inclusions inside a silicon dioxide matrix. The lattice constant *a* is 2.5 μm in the x and y directions and the tungsten rods have radii of 0.6 μm. The thickness of the PnCs is 1.85 μm. To model an infinite periodic structure along y direction, periodic boundary conditions are employed on the bottom and top nodes. The exterior domains, shown in Fig 1 , comprises perfectly matched layers (PMLs). The PMLs serve to attenuate the outgoing waves, and reflect little to no energy back into the PnC[6]. Longitudinal waves are launched into the PnC by harmonic excitation of the nodes on the left surface of the leftmost exterior domain (See Fig. 1). In the 2D, model all the dimensions are similar to the shown 3D model but the numerical space is a 2D rectangle due to plane stress assumptions.

Material	Tungsten	Silicon dioxide
Density (kg/m^3)	19250	2200
Young's Modulus (GPa)	409	75
Poisson's Ratio	0.25	0.17

Table 1 Materials that constitute the PnC.

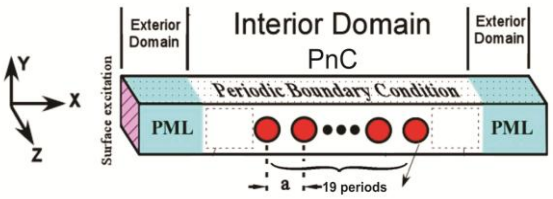

Figure 1 Numerical space of the 3D model for the PnC.

In Table 1 the density, elastic modulii, and Poisson's ratios of silicon dioxide and tungsten are shown. In the 3D simulation, only extensional elastic waves are taken into account, in order to make more accurate comparison to the

Phononics 2011: First International Conference on Phononic Crystals, Metamaterials and Optomechanics
Santa Fe, New Mexico, USA, May 29-June 2, 2011
PHONONICS-2011-0152

2D case in which no flexural modes are allowed. For this reason only symmetric forces are applied on the boundary condition of the left exterior domain (see Fig 1).

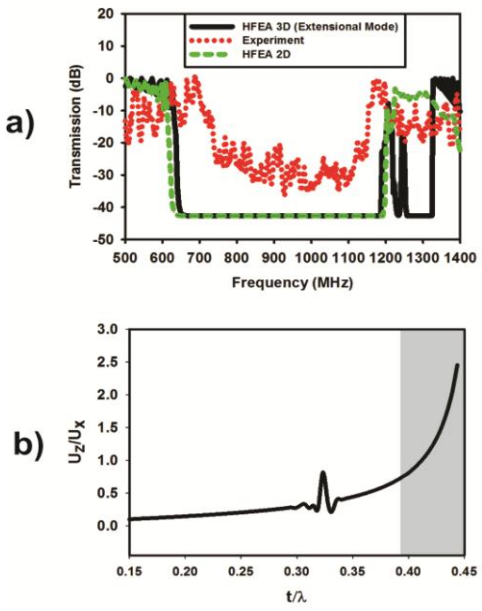

Figure 1 (a) Transmission spectrum based on the 2D HFEA (red dotted line), 3D HFEA (green dashed line), and the experiment (red dotted line). **(b)** Ratio of out-of-plane to in-plane displacements versus dimensionless excitation frequency. The shaded gray region indicates the frequencies at which the 2D and 3D finite elements analyses do not agtree.

The scaled transmission of the PnC predicted by the FEA using 2D and 3D approaches are presented in Fig. 2a. In this plot HFEA 2D stands for the prediction of a 2D elastodynamic model for the transmission through the PnC. The 3D simulation is compared with the 2D model along with the actual experimental results previously reported by Su et al.[3]. Here, the borders of bandgp are defined by transmission of -10 (dB). The comparison shows that both finite element models predict a similar primary bandgap. The predicted beginning frequency is about 80 MHz smaller than the experimental prediction. Moreover, the actual end frequency of the band gap is only 20 MHz smaller than the numerical results, which shows a good agreement between the theoretical 2D, theoretical 3D, and experimental piramary bandgaps. However, Fig. 2a also demonstrates that the 2D model fails to predict the experimental secondary bandgap ranging from 1180 MHz to 1400 MHz. In contrast to the 2D model, the 3D model clearly shows this band gap.

The discrepancy between the 2D and 3D analyses at the higher frequencies raises the question of validity of the 2D analysis. This question is addressed in Fig. 2b. Here, the ratio of out-of-plane displacement (U_z) to the in-plane displacement (U_x) on the right side of the PnC (See Fig 1) is depicted for different dimensionless frequencies defined as the ratio of the PnC thickness t to the wavelength λ. Additionally, this dimensionless frequency in the abscissa of Fig. 2b corresponds to the frequency in abscissa of Fig 2a. The shaded region in Fig. 2b shows the dimensionless frequencies corresponding to the secondary band gap where the two dimensional FEA is not in agreement with the experiment and 3D model. One can notice that in the shaded box the three dimensional FEA shows a range from 0.7 and 2.5 for the ratio of out-of-plane to in-plane displacements. This high ratio indicates that the out-of-plane displacements are not insignificant in the problem while the 2D analysis inherently does not take these displacements into account. It also indicates that the nature of the problem is not 2D at the frequencies associated with the secondary bandgap. The trend of dimensionless lateral displacements shown in Fig. 2b suggests that the 2D analysis is not applicable when the ratio of the thickness to wavelength approaches to 0.5. Another physical explanation is that when the wavelength approaches to half of the thickness, the out-of-plane mode of vibration is greatly excited because the excitation frequency is close to the natural frequency of this mode. However at lower frequencies the 2D and 3D analyses do not show a significant difference. In essence, Fig 1 suggests that at the dimensionless excitation frequencies much smaller than 0.37 the 2D HFEA is an accurate alternative to 3D the model. Since a 2D model requires a smaller numerical space, one might consider attaining a fast approximation of a phononic bandgap, when the wavelength is much greater than half of the thickness.

References

[1] I. Olsson III, R. H., and El-Kady, I. F., *Measurement Science and Technology* **20**, 012002 (2008).
[2] Saad, M., H., *Elasticity, Theory, Applications, and Numerics*, Academic Press, USA (2004).
[3] Su, M. F., Olsson III, R. H., Leseman, Z. C., El-Kady, I. F., *App. Phys. Lett.* **96**, 053111 (2010).
[4] Hussein, M. I., Hulbert, G. M., Scott, R. A., *Journal of Sound and Vibration* **307**, 865-893 (2007).
[5] Jensen, J. S., *Journal of Sound and Vibration* **301**, 319-340 (2007).
[6] Basu, U., Chopra, A. K., *Comput. Methods Appl. Mech. Eng*. **192**, 1337–1375 (2003).

Phononics 2011: First International Conference on Phononic Crystals, Metamaterials and Optomechanics
Santa Fe, New Mexico, USA, May 29-June 2, 2011
PHONONICS-2011-0155

From Newton's Cradle to New Acoustic Crystals

Chiara Daraio

Engineering and Applied Sciences, California Institute of Technology, 1200 E California Blvd. Pasadena CA 91125, USA. Daraio@caltech.edu

Abstract: The bouncing beads of Newton's cradle fascinate children and executives alike, but their symmetric dance hides a complex dynamic behavior. By assembling grains in crystals we are developing new materials and devices with unique properties. We have constructed two-dimensional systems that can redirect mechanical waves, and have developed new materials for absorbing vibrations and explosive blasts.

In this paper, I will discuss recent progress obtained in the study of nonlinear acoustic crystals. In particular, I will discuss the response of granular crystals excited by impulsive loading and continuous vibrations. Granular crystals are here defined as highly ordered aggregates of particles in elastic contact with each other, preferably in linear or network shaped arrangements. In our work, the assemblage of the novel acoustic materials is achieved by aligning granular components inside a selected matrix (Fig. 1) or in a self-standing crystal, designing contact interactions for the control of stress transfer between particles. The design of these materials starts from a well-understood local phenomenon (i.e. the elastic Hertzian contact interactions between particles) and creates global structures with unique properties (the granular crystals). This work leverages theoretical understanding of the highly nonlinear dynamic response of the fundamental components[1] for the design of experiments, and it is informed by discrete numerical simulations. The potential applications targeted by our work are: i) mechanical systems with tunable acoustic/elastic properties; ii) devices with controllable acoustic bandgaps within the audible range, noise mitigation and vibration absorbing layers; iii) novel shock-energy-trapping and pulse-disintegrating devices and micro- or macro-impact shielding; iv) new acoustic lenses with a tunable focal point and v) new methods of Non Destructive Evaluation, Structural Health Monitoring (NDE/SHM) and modal testing. In this paper, I will focus on recent results obtained with two-dimensional granular systems excited by impulsive loading and continuous vibrations. I will present how granular crystals can control the propagation of acoustic waves by varying the static compression applied to the system, the particles' geometry and material properties.

Figure 1 (Left) Example of a three-dimensional acoustic crystal realized aligning 2mm φ beads in vertical lodgings in a soft polymer matrix[2]; (right) zoomed in view from top.

Background

A chain of spherical particles (i.e. a longer version of the well known "Newton's cradle" toy) hides an intriguing elegant complexity, and a myriad of tunable mechanical phenomena that have been attracting increasing attention in the scientific community[1-6]. Some of the earliest findings in this discrete system[1-4] reported the formation of new, highly nonlinear solitary waves, with a finite wavelength, when the system is impacted at one end by a striker. The presence of defects and impurities has been shown to cause scattering and energy trapping[5]. When the system is highly precompressed its response can be varied to become weakly nonlinear or linear, depending on the ratio between the dynamic excitations' amplitude and the amplitude of the static compressive force[3]. When these systems are driven in the linear or weakly nonlinear regime, they present tunable band gaps in their dispersion relation[6]. In our current work, we have extended these findings to two-dimensional systems[7] (Fig. 2) composed of uniform and heterogeneous materials.

Phononics 2011: First International Conference on Phononic Crystals, Metamaterials and Optomechanics
Santa Fe, New Mexico, USA, May 29-June 2, 2011
PHONONICS-2011-0155

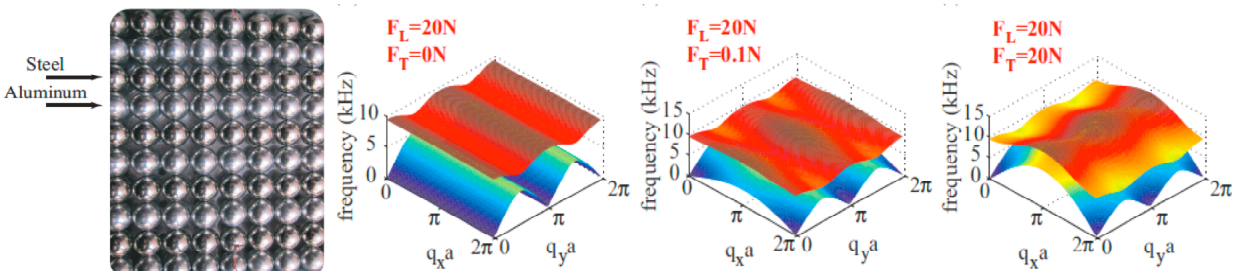

Figure 2 (Left) Two-dimensional acoustic crystal realized aligning steel and aluminium particles in alternating layers. (right) Dispersion relations calculated for a constant longitudinal static force (F_L = 20N) and a transversal force (F_T) taking the values 0, 0.1 and 20N.

studied periodic arrays of particles with variable precompression using theory, discrete numerical models and experiments. We consider different configurations of the lattices, using spheres made of different materials. Experimental measurements of the transmitted power spectral density are performed highlighting the presence of band gaps in two-dimensional diatomic (two-particle periodicity, Fig. 2) or triatomic crystals. Depending on the static force applied, the edge frequency of the acoustic and optical bands can be tuned. In the layered diatomic square packing studied, when the static transversal force is equal to 0, a quasi one-dimensional response is observed. When the static transversal force is increased, the propagation of waves can be tuned from 1-D to 2-D, enabling transversal energy propagation. These systems could be used as tunable, load-bearing vibration absorbers or acoustic filters for frequencies belonging to the audible range.

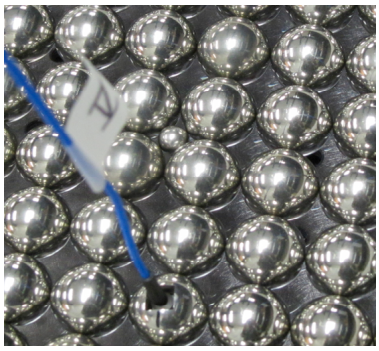

Figure 3 Digital image of the experimental setup used to study the effect of a defect in a 2-D squared array of stainless steel particles. The image shows the interstitial defect and one of the triaxial accelerometers embedded in a particle to detect the waves.

We also study the effects of defects in a squared packing of uniform particles, when the system in non-precompressed and excited by transient pulses. The defect corresponds to an interstitial impurity of different materials (Fig. 3). We analyze the response of the traveling signal as a function of the materials properties for the defect particles and study the resulting energy trapping, redirection and particles oscillations. The defects behave as energy scatterers and, depending on their materials properties, can trap variable amount of energy and momentum. The interaction of multiple defects on the same lattice will also be discussed. The work includes experiments and numerical simulations based on a discrete particle model.

Future developments will include the use of numerical optimization to control wave propagation and energy transmission selecting optimal particles' geometry, materials and arrangements.

Acknowledgements
The work described in this extended abstract has been performed in collaboration with Dr. Stephane Griffiths and Mr. Ivan Szelengowicz at Caltech. The work was supported by Office of Naval Research - YIP, by the United Technologies Research Center, and by an ARO/MURI.

References

[1] Nesterenko, V.F., *Dynamics of Heterogeneous Materials*., NY, Springer−Verlag (2001).
[2] Daraio, C.; Nesterenko, V.F.; Jin, S.; APS - Shock Compression of Condensed Matter, 197-200, American Institute of Physics, Conference Proceedings, Portland (OR), (2003).
[3] Daraio, C.; Nesterenko, V.F.; Herbold, E.; Jin, S. *Physical Review E*, 73, 026610, (2006).
[4] Sen, S. et al. *Physics Reports* 462, 21–66, (2008).
[5] S. Job, et al. *Phys. Rev. E* 80, 025602(R), (2009).
[6] Herbold, E.B. et al. *Acta Mechanica* 205, 1-4, 85-103, (2009).
[7] Gilles, B., Coste, C. Powders and Grains, 4th International Conference on Micromechanics of Granular Media, (2001).

Phononics 2011: First International Conference on Phononic Crystals, Metamaterials and Optomechanics

Santa Fe, New Mexico, USA, May 29-June 2, 2011

PHONONICS-2011-0163

Acoustic Logic Gates Implemented Using A Phase Controlling Phononic Crystal

Stefan Bringuier[1] , Nichlas Z. Swinteck[1], Jerome O. Vasseur[2], Jean-Francois Robillard[2], Keith Runge, Krishna Muralidharan[1], Pierre Deymier[1]

[1] University of Arizona, AZ, USA
stefanb@email.arizona.edu, swinteck@email.arizona.edu, krishna@email.arizona.edu, deymier@email.arizona.edu
[2] Institut d'Electronique, de Micro-electronique et de Nanotechnologie, France
jerome.vasseur@univ-lille1.fr, Jean-Francois.Robillard@isen.fr
krunge@bellsouth.net

Abstract: A Phononic crystal (PC) consisting of a square array of cylindrical Polyvinylchloride inclusions in air, is used to construct a variety of acoustic logic gates. This PC has a unique band structure that allows for the control of the relative phase between incident acoustic waves. The realization of the gates is demonstrated through simulations employing the finite-difference-time-domain method.

Phononics 2011: First International Conference on Phononic Crystals, Metamaterials and Optomechanics

Santa Fe, New Mexico, USA, May 29-June 2, 2011

PHONONICS-2011-0163

Phononics 2011: First International Conference on Phononic Crystals, Metamaterials and Optomechanics
Santa Fe, New Mexico, USA, May 29-June 2, 2011
PHONONICS-2011-0165

Device Level Harmonic Finite Element Analysis of Phononic Crystals Operating at GHz Frequencies

S. Alaie[1], I. El-Kady[2], and Z. C. Leseman[1*]

[1] *Mechanical Engineering, University of New Mexico, Albuquerque, NM USA 87131*
alaie@unm.edu, and zleseman@unm.edu
[2] *Sandia National Laboratories, Albuquerque, NM USA 87105*
ielkady@sandia.gov

Abstract: The vibrational behavior of a phononic crystal is studied at gigahertz frequencies. The phononic crystal is comprised of a silicon slab with tungsten inclusions filtering out waves within the frequency range of 0.7 GHz to 1.1 GHz. Comparisons show that the harmonic finite element analysis is capable of more accurately explaining the experimental results than FDTD when compared to experiments.

For this poster, the vibrational behavior of a phononic crystal is studied at gigahertz frequencies. The phononic crystal is comprised of a silicon slab with tungsten inclusions filtering out waves within the frequency range of 0.7 GHz to 1.1 GHz. Two-dimensional harmonic finite element analysis (FEA) is employed to model the transmission of stresswaves launched from a transmitter and passing through the crystal. The numerical results are compared with another prevalent numerical method, finite difference time domain (FDTD), as well as with experimental results. These comparisons show that the harmonic finite element analysis is capable of more accurately explaining the experimental results than FDTD. This more favorable comparison is attributed to a resonance that course between the transmitter and the phononic crystal.

Phononics 2011: First International Conference on Phononic Crystals, Metamaterials and Optomechanics

Santa Fe, New Mexico, USA, May 29-June 2, 2011

PHONONICS-2011-0165

Phononics 2011: First International Conference on Phononic Crystals, Metamaterials and Optomechanics
Santa Fe, New Mexico, USA, May 29-June 2, 2011
PHONONICS-2011-0173

Phononic Band Gap Optimization for Combined In-Plane and Out-of-Plane Waves

Osama R. Bilal, Mahmoud I. Hussein

Department of Aerospace Engineering Sciences, University of Colorado at Boulder, CO 80309, USA
osama.bilal@colorado.edu, mih@colorado.edu

Abstract: Utilizing the reduced Bloch mode expansion method for fast band structure calculations and specialized genetic algorithms for a search among numerous topologies, optimal phononic crystal unit cell designs are generated for (1) in-plane, (2) out-of-plane and (3) combined in-plane and out-of-plane elastic wave propagation in a 2D geometrically periodic *single material* media. This process of natural evolution yields elegant designs with exceptionally large, and low, frequency band gaps.

Phononic crystals are material systems with the distinct feature of unit cell repetition. The unit cell is composed of at least two types of material phases with different properties or a single material with a non-uniform geometric structure. An important dispersion-related characteristic of wave propagation through phononic crystals is the existence of frequency band gaps, where waves do not propagate. The widths of these bands, and their locations in the frequency domain, depend on the topology of the unit cell, material-wise or geometry-wise. Through topology optimization, the configuration of the unit cell can be designed to exhibit a maximum value of band gap width divided by band gap central frequency, i.e., *large and low band gap*. This problem has been investigated earlier for bi-material media with a focus on either in-plane (P/SV) wave propagation or out-of-plane (SH) wave propagation[1-3]. In this paper we consider geometrically periodic square lattices formed from only one material (silicon), and investigate three band-gap optimization problems: (1) in-plane waves only, (2) out-of-plane waves only and (3) combined in-plane and out-of-plane waves.

We build our elastodynamic model based on the wave equation for a two-dimensional media under plain strain conditions[1,4]. In this model, incident in-plane waves travel at the speed of the material's longitudinal velocity c_l and incident out-of-plane waves travel at the speed of the material's transverse velocity c_t. The phononic band structure is calculated by employing Bloch theory and using the finite element method to expand the equation of motion in real space. Furthermore, the reduced Bloch mode expansion (RBME) method[3] is used to substantially reduce the size of the computational model and hence make it feasible to search, using genetic algorithms (GA), among an exceedingly large design space representing a multitude of different possible material distributions within the unit cell domain.

Unit Cell Representation and Design Objective

The square unit cell Y is composed of $n \times n$ pixels forming a matrix G, which we reduce in size following the underlying lattice symmetry. Each of the pixels can be assigned to either a *no material* or a *material* (silicon), i.e., $g_{ij} \in \{0,1\}$. We formulate our objective function in terms of the size of a particular band gap normalized with respect to its central frequency:

$$f(g) = \frac{max\,(min_{j=1}^{n_k}(\omega_{i+1}^2(k_j,g)) - max_{j=1}^{n_k}(\omega_i^2(k_j,g)),0)}{(min_{j=1}^{n_k}(\omega_{i+1}^2(k_j,g)) + max_{j=1}^{n_k}(\omega_i^2(k_j,g)))/2}, \quad (1)$$

where $min_{j=1}^{n_k}(\omega_i^2(k_j,g))$ and $max_{j=1}^{n_k}(\omega_i^2(k_j,g))$ denote the minimum and maximum, respectively, of the i^{th} frequency ω_i over the entire discrete wave vector set, k_j, $j=1,\ldots,n_k$, tracing the border of the irreducible Brillouin zone.

Genetic Algorithm

For the initialization step in the GA, we observed that almost any randomly generated design at high unit cell resolution (i.e. $n \geq 24$ pixels) exhibits no band gap. To address this problem, we use the area

Phononics 2011: First International Conference on Phononic Crystals, Metamaterials and Optomechanics
Santa Fe, New Mexico, USA, May 29-June 2, 2011
PHONONICS-2011-0173

between the two dispersion branches of interest as an indicator for the fitness of the unit cell designs used in the GA selection operation:

$$Fitness = \phi f(g) + F \tag{2}$$

$$F = \begin{cases} 0 & \text{if } f(g) > 0 \text{ (band gap exists)} \\ Area & \text{if } f(g) = 0 \text{ (no band gap)} \end{cases}, \tag{3}$$

$$Area = \sum_{j=1}^{n_k} [(\omega_{i+1}^2(k_j, g)) - (\omega_i^2(k_j, g))]. \tag{4}$$

In Eq. (2), ϕ is chosen to be a large number $(\phi = 10^4)$ in order to guarantee that any design that has a band gap is selected over a design that has no band gap. Furthermore, the GA initialization procedure is set to ensure that each two adjacent pixels in a row have the same material type. At each evolutionary step, a simple single point crossover is carried out between the two selected designs with a tournament selection operator. Finally the GA is programmed to terminate when the generation counter reaches the max number of generations. Following termination, the best surviving design passes through a simple one-point flip local search for fine-tuning.

Results and Conclusion

Upon implementing our GA- and RBME-based search methodology, we obtained the following optimal unit cell designs. Fig. (1): first band gap for out-of-plane waves, band gap size f = 0.7884; Fig. (2): second band gap for out-of-plane waves, band gap size f = 0.8945; Not shown: first band gap for in-plane waves, band gap size f = 0; Fig. (3): second band gap for in-plane waves, band gap size f = 0.8705; Fig. (4): lowest possible band gap for combined out-of plane and in-plane waves; band gap size f^* = 0.6938, where the superscript "*" denotes a modified objective function that describes maximization of a combined band gap among the band structures of the two types of waves. We note that the out-of-plane designs show a continuous solid media approaching the limiting case of separate square inclusions in air. The in-plane designs on the other hand show a mostly solid material with delicately shaped air holes. The optimal design for the combined case appears to be a blend among the out-of-plane and in-plane design traits. All designs are amenable to fabrication upon post-optimization smoothening.

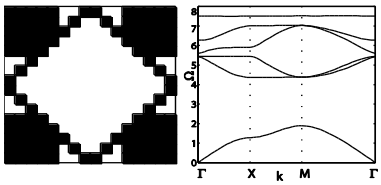

Figure 1. Optimal design for 1st band gap for out-of-plane waves

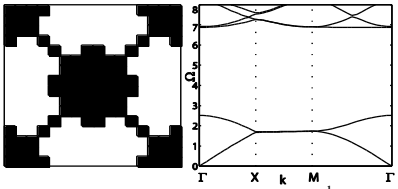

Figure 2. Optimal design for 2nd band gap for out-of-plane waves

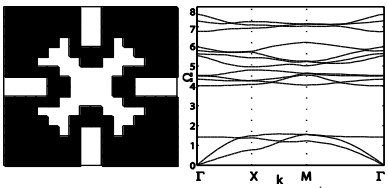

Figure 3. Optimal design for 1st band gap for out-of-plane waves

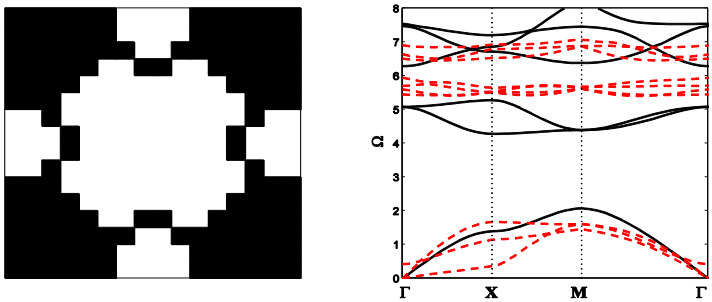

Figure 4. Optimal design for combined in-plane (red-dashed) and out-of-plane (black) waves

References

[1] O. Sigmund and J.S. Jensen, *Philosophical Transactions of the Royal Society A*. **361**, 1001-1019 (2003).
[2] M. I. Hussein, K. Hamza, G. M. Hulbert, and K. Saitou, *Waves in Random and Complex Media*, **17**, 491-510 (2007).
[3] M. J. Rupp, A Evgrafov, K. Maute and M. L. Dunn, *Structural and Multidisciplinary Optimization*, **34**, 111-122 (2007).
[4] M. I. Hussein, *Proceedings of the Royal Society A*. **465**, 2825-2848 (2009).

Phononics 2011: First International Conference on Phononic Crystals, Metamaterials and Optomechanics
Santa Fe, New Mexico, USA, May 29-June 2, 2011
PHONONICS-2011-0182

Multiscale Dispersive Design: A Building Blocks Approach to Phononics

Mahmoud I. Hussein

Department of Aerospace Engineering Sciences, University of Colorado at Boulder, CO 80309, USA
mih@colorado.edu

Abstract: A key feature in most applications in phononics is an underlying spatial periodicity. When infinite in extent, this spatial symmetry constitutes a periodic "material". When truncated to finite dimensions, a periodic "structure" is formed. Between the two entities there is an abundance of opportunities for shaping a desired wave propagation or vibration response. In this work we will revisit the concept of Multiscale Dispersive Design and use it towards the exploration of new avenues in phononic crystals and metamaterials applications.

Within phononic crystals and metamaterials, various wave phenomena occur across the underlying spatial periodicity inducing mechanisms of wave interference and/or local resonance that lead to a banded frequency response. Similar physical behavior is possible within finite structures composed of periodic materials although the periodicity truncation in itself alters the dynamical characteristics (see, e.g., Ref. 1). In some cases these alterations are mild (for example, the frequency range of the band gaps are practically retained), but in other cases significant changes to the dynamical response are realized, such as the possible appearance of resonances in the band gap. It has been shown in several studies that if a substantially large number of unit cells is retained in the truncated structure, or the finite periodic material portion of a structure, then the frequency response of the underlying unit cell will still dominate[1].

In this paper, we will revisit the concept of Multiscale Dispersive Design (MDD) previously proposed by the author and collaborators[2,3]. This is essentially a design methodology whereby periodic unit cells are designed for desired frequency band properties, and with appropriate scaling, these cells are used as *building blocks* for forming fully periodic or partially periodic structures with related dynamical characteristics. Through this approach, which is hierarchical and integrated, structures can be devised for a wide range of wave propagation and vibration response tailored to specification.

As an example we consider the problem of designing a passive demultiplexer using phononic crystals, a problem previously studied in the literature[4]. From Ref. 3, Fig. 1 shows a two-dimensional plate-like structure formed from three types of phononic crystal building blocks each based on a unit cell with a unique band gap: the group of cells with a black inclusion function as "walls" for all waves in the frequency range of $3 \le \Omega \le 4$ (Ω denotes non-dimensional frequency), and the group of cells with an orange or a blue inclusion functions as a "gate" that allow passage of waves in the range of $3.4 \le \Omega \le 4$ or $3 \le \Omega \le 3.8$, respectively. By employing a portion of each type of periodic material (i.e., with at least 3-4 unit cells in each direction), the underlying band gap properties will still take effect in the truncated configuration. In this manner a passive demultiplexer is formed by the macroscale layout shown in Fig. 1.

The building blocks approach demonstrated by this demultiplexer example is being extended to a variety of new applications in phononics. A description and analysis of these applications and their potential impact to the engineering of novel devices, or coupled material/structure systems, will be discussed.

Phononics 2011: First International Conference on Phononic Crystals, Metamaterials and Optomechanics
Santa Fe, New Mexico, USA, May 29-June 2, 2011
PHONONICS-2011-0182

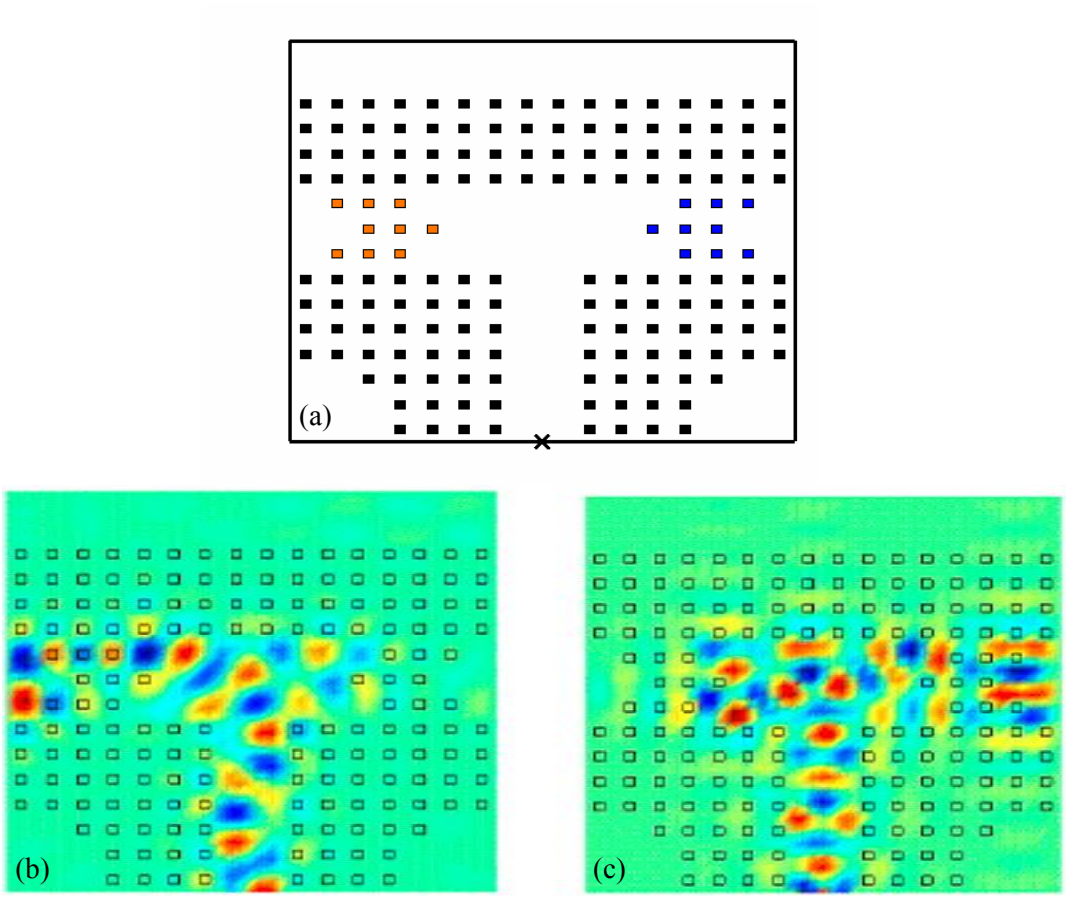

Figure 1. (a) Frequency demultiplexer formed from a combination of phononic crystal building blocks. In this passive structure, low frequency waves are turned to the left (b), and high frequency waves are turned to the right (c).

References

[1] M. I. Hussein, G. M. Hulbert and R. A. Scott, *Journal of Sound and Vibration*, **289**, pp. 779-806 (2006).
[2] M. I. Hussein, G. M. Hulbert and R. A. Scott, *Journal of Sound and Vibration*, **307**, pp. 865-893 (2007).
[3] M. I. Hussein, G. M. Hulbert and R. A. Scott, ASME IMECE 2005, Paper IMECE2005-81325, pp. 1-10 (2005).
[4] Y. Pennec, B. Djafari-Rouhani, J. O. Vasseur, A. Khelif, P. A. Deymier, *Physical Review E*, **69**, 046608 (2004).